TRW

TAPCO GROUP

Thompson Ramo Wooldridge Inc.

Cleveland 17, Ohio

DISCLAIMER

MND-P-2376
ENGINEERING REPORT 4051

SNAP I POWER CONVERSION SYSTEM TURBINE DEVELOPMENT

PREPARED BY

NEW DEVICES LABORATORIES, TAPCO GROUP
THOMPSON RAMO WOOLDRIDGE INC.

AS AUTHORIZED BY

THE MARTIN CO. PURCHASE ORDER NO. 0E 0101

FOR

THE UNITED STATES ATOMIC ENERGY COMMISSION
PRIME CONTRACT AT(30-3)-217

1 FEBRUARY 1957 TO 30 JUNE 1959

PUBLISHED 20 JUNE 1960

PREPARED BY:

D. C. REEMSNYDER
E. M. SZANCA

LEGAL NOTICE

This report was prepared as an account of Government sponsored work. Neither the United States, nor the Commission, nor any person acting on behalf of the Commission:

A. Makes any warranty or representation, expressed or implied, with respect to the accuracy, completeness, or usefulness of the information contained in this report, or that the use of any information, apparatus, method, or process disclosed in this report may not infringe privately owned rights; or

B. Assumes any liabilities with respect to the use of, or for damages resulting from the use of any information, apparatus, method, or process disclosed in this report.

As used in the above, "person acting on behalf of the Commission" includes any employee or contractor of the Commission to the extent that such employee or contractor prepares, handles or distributes, or provides access to, any information pursuant to his employment or contract with the Commission.

DISTRIBUTION LIST

		Copy No.
1.	Commander, AFBMD Hq., USAF ARDL P.O. Box 262 Inglewood, California For: Maj. G. Austin	1
2.	Commander, ARDC Andrews Air Force Base Washington 25, D. C. Attn: RDTAPS, Capt. W. G. Alexander	2
3.	Army Ballistic Missile Agency Commanding General Army Ballistic Missile Agency Redstone Arsenal, Alabama Attn: ORDAB-c	3, 4
4.	U. S. Atomic Energy Commission Technical Reports Library Washington 25, D. C. Attn: Mr. J. M. O'Leary For: Lt. Col. G. M. Anderson, DRD Capt. John P. Wittry, DRD Lt. Col. Robert D. Cross, DRD R. G. Oehl, DRD Edward F. Miller, PROD Technical Reports Library	5 through 10
5.	Atomics International Division of North American Aviation, Inc. P. O. Box 309, Canoga Park, California Attn: Dr. Chauncey Starr For: J. Wetch	11
6.	Chief, Bureau of Aeronautics Washington 25, D. C. Attn: C. L. Gerhardt, NP	12

DISTRIBUTION LIST (Continued)

		Copy No.
7.	Chief, Bureau of Ordnance Dept. of the Navy, 4110 Main Navy Bldg. Washington 25, D. C. Attn: Mrs. R. Schmidt or G. Myers To be opened by addressee only for: Ren, SP	13, 14
8.	Chief, Bureau of Ships Department of the Navy, Code 1500 Washington 25, D. C. Attn: Melvin L. Ball	15
9.	U. S. Atomic Energy Commission Canoga Park Area Office P. O. Box 591 Canoga Park, California Attn: A. P. Pollman, Area Manager	16
10.	U. S. Atomic Energy Commission Chicago Operations Office P. O. Box 59, Lemont, Ill. Attn: A. I. Mulyck For T. A. Nemzek, Mr. Klein	17, 18
11.	Office of the Chief of Naval Operations Department of the Navy Washington 25, D. C.	19
12.	Atomic Division Office of Chief of Research & Development Department of the Army Washington 25, D. C.	20
13.	Commanding Officer Diamond Ordnance Fuse Laboratories Washington 25, D. C. Attn: ORDTL 06.33, Mrs. M. A. Hawkins	21 through 23

DISTRIBUTION LIST (Continued)

		Copy No.
14.	U. S. Atomic Energy Commission Hanford Operations Office P. O. Box 550 Richland, Washington Attn: Technical Information Library	24
15.	Lockheed Aircraft Corporation Missile Systems Division Palo Alto, California Attn: Mr. Hal H. Greenfield	25, 26
16.	Monsanto Chemical Company Mound Laboratory P. O. Box 32, Miamisburg, Ohio Attn: Library and Records Center For: Mr. Roberson	27
17.	National Aeronautics & Space Administration Ames Aeronautical Laboratory Moffett Field, California Attn: Smith J. de France, Director	28
18.	National Aeronautics & Space Administration Langley Aeronautical Laboratory Langley Field, Virginia Attn: Henry J. E. Reid, Director	29
19.	National Aeronautics & Space Administration Lewis Flight Propulsion Laboratory 21000 Brookpark Road Cleveland 35, Ohio Attn: George Mandel	30
20.	Commander U. S. Naval Ordnance Laboratory White Oak, Silver Spring, Maryland Attn: Eva Lieberman, Librarian	31 through 33

DISTRIBUTION LIST (Continued)

		Copy No.
21.	Director Naval Research Laboratory, Code 1572 Washington 25, D. C. Attn: Mrs. Katherine H. Cass	34
22.	U. S. Atomic Energy Commission New York Operations Office 376 Hudson Street New York 14, New York Attn: Reports Librarian	35, 84
23.	Union Carbide Nuclear Company X-10, Laboratory Records Department P. O. Box X Oak Ridge, Tennessee Attn: Eugene Lamb	36
24.	Office of Naval Research Department of the Navy, Code 735 Washington 25, D. C. Attn: E. E. Sullivan For: Code 429	37
25.	Director, USAF Project Rand Via AF Liaison Of., The Rand Corporation 1700 Main St., Santa Monica, California Attn: F. R. Collbohm For: Dr. J. Huth	38
26.	Commander, Rome Air Development Center Griffiss Air Force Base, New York Attn: RCSG, J. L. Briggs	39
27.	U. S. Atomic Energy Commission Reference Branch Technical Information Service Extension Oak Ridge, Tennessee	40 through 64

DISTRIBUTION LIST (Continued)

		Copy No.
28.	Thompson Ramo Wooldridge Staff Research and Development New Devices Laboratories P. O. Box 1610, Cleveland 4, Ohio	65, 66, 67
29.	Univ. of Calif. Radiation Lab Technical Information Division P. O. Box 808, Livermore, Calif. Attn: C. G. Craig For: Dr. H. Gordon	68
30.	Commander, Wright Air Dev. Center Wright-Patterson Air Force Base, Ohio Attn: WCACT For: Capt. N. Munson, WCLPS, G. W. Sherman, WCLEE, WCOSI	69 through 72
31.	Commanding Officer Jet Propulsion Laboratory Pasadena, California Attn: W. H. Pickering, I. E. Newlan	73
32.	Univ. of California Radiation Lab Technical Information Division P. O. Box 808, Livermore, California Attn: Clovis G. Craig For: Dr. Robert H. Fox	74
33.	Los Alamos Scientific Laboratory P. O. Box 1663 Los Alamos, New Mexico Attn: Report Librarian For: Dr. George M. Grover	75
34.	Commander Air Force Special Weapons Center Technical Information & Intelligence Office Kirtland Air Force Base, New Mexico Attn: Kathleen P. Nolan	76

DISTRIBUTION LIST (Continued)

		Copy No.
35.	School of Aviation Medicine Brooks Air Force Base, Texas	77
36.	Commander Aero-space Technical Intelligence Center Wright-Patterson Air Force Base, Ohio Attn: H. Holzbauer, AFCIN-4 Bia	78
37.	National Aeronautics & Space Administration 1512 H. Street, N. W., Washington 25, D. C. Attn: Dr. Addison M. Rothrock	79 through 83
38.	The Martin Company P. O. Box 5042, Baltimore 20, Maryland Attn: AEC Document Custodian	86 through 90
39.	Advanced Research Project Agency The Pentagon, 3D154, Washington 25, D. C. Attn: Fred A. Koether or Donald E. Percy	85

FOREWORD

SNAP I is the first of a family of devices to convert nuclear energy to electrical for use in space. The SNAP Systems for Nuclear Auxiliary Power - programs are sponsored by the Atomic Energy Commission; the SNAP I prime contractor is The Martin Company. SNAP I was designed to utilize a radio isotope as the energy source.

The SNAP I Power Conversion System utilizes mercury as the working fluid for a Rankine cycle. A radioisotope is used as the energy source to vaporize mercury in a boiler; turbo-machinery extracts the useful energy from the vapor and converts it into electrical energy; the exhaust vapor is condensed by rejecting the waste thermal energy to space in a condenser-radiator.

During the SNAP I Power Conversion System development, Thompson Ramo Wooldridge has been responsible for the development of the following items:

Turbo-machinery

- Mercury vapor turbine
- Alternator
- Lubricant and condensate pump
- Mercury lubricated bearings

Speed Control

Condenser-Radiator

A series of eight Engineering Reports have been prepared describing Thompson Ramo Wooldridge's SNAP I Power Conversion System development program. These are as follows:

ER-4050	Systems
ER-4051	Turbine
ER-4052	Alternator
ER-4053	Pump
ER-4054	Bearings
ER-4055	Control
ER-4056	Condenser-Radiator
ER-4057	Materials

The material in this report deals specifically with the developmental history of the turbine for the SNAP I Power Conversion System. This report is submitted as part of the requirements of Purchase Order OE-0101 from the Martin Company, issued under the Atomic Energy Commission prime contract AT(30-3)-217.

TABLE OF CONTENTS

1.0 SUMMARY

The SNAP I mercury vapor turbine development program included analysis, design, fabrication and testing of several types of turbines in order to determine feasibility, obtain experimental results, and select a turbine capable of meeting the design specifications.

Preliminary analytical and experimental investigations of the regenerative-type turbines (drag and vortex) indicated that these turbines were relatively low efficiency machines, and extensive development would have been necessary to obtain the required design efficiency of 40%. Final analytical and experimental development was conducted on the axial flow impulse turbine due to the advanced state-of-the-art of this type turbine.

The final SNAP I turbine consisted of a three stage, axial flow, impulse, mercury vapor turbine with the first two stages having partial admission and the third stage having full admission. Basic considerations in the turbine design were reliability, weight, size, efficiency, performance, erosion, external leakage, life, and system integration.

Experimental results verified that the SNAP I axial flow, mercury vapor turbine successfully attained the design efficiency requirement of 40%; the over-all design point turbine efficiency obtained was 42 percent. The SNAP I power conversion system demonstrated the design 60 day life in a system endurance test. The system accumulated 2510 hours of operation with no deterioration of turbine performance.

Analytical and empirical axial flow turbine design procedures were evolved and verified by experimental air and mercury vapor testing for low power output, high pressure ratio, high speed, mercury vapor turbines. Digital computer programs were also utilized in the analysis, design, and experimental evaluation of the SNAP I axial flow turbine.

A completely equipped air and steam Turbine Test Facility was designed and fabricated for cold and hot gas testing of small turbines.

2.0 INTRODUCTION

Figure 2-1 shows the turbomachinery package of SNAP I, the first space power plant. This unique subminiature electric power generator contains the turbine, alternator, and condensate pump for the Rankine cycle power conversion system. These components are mounted on a common shaft rotating at 40,000 rpm and supported by mercury lubricated bearings.

Because it is required to operate unattended for long durations in stringent environmental conditions, the SNAP I turbomachinery package is the result of advanced engineering concepts in analysis, design, fabrication, and experimentation.

This report describes the development of the mercury vapor turbine for this package.

The SNAP I mercury vapor turbine was required to operate at a very high pressure ratio in order to optimize the Rankine cycle efficiency. Considerations of the high pressure ratio, low power output, small size, and the requirements of high reliability, and efficiency indicated that extrapolation of empirical turbine design constants would be required.

A turbine development program was established to determine the feasibility, correlate analytical and experimental results, and develop a turbine capable of meeting the system design specifications.

SNAP I TURBOMACHINERY PACKAGE

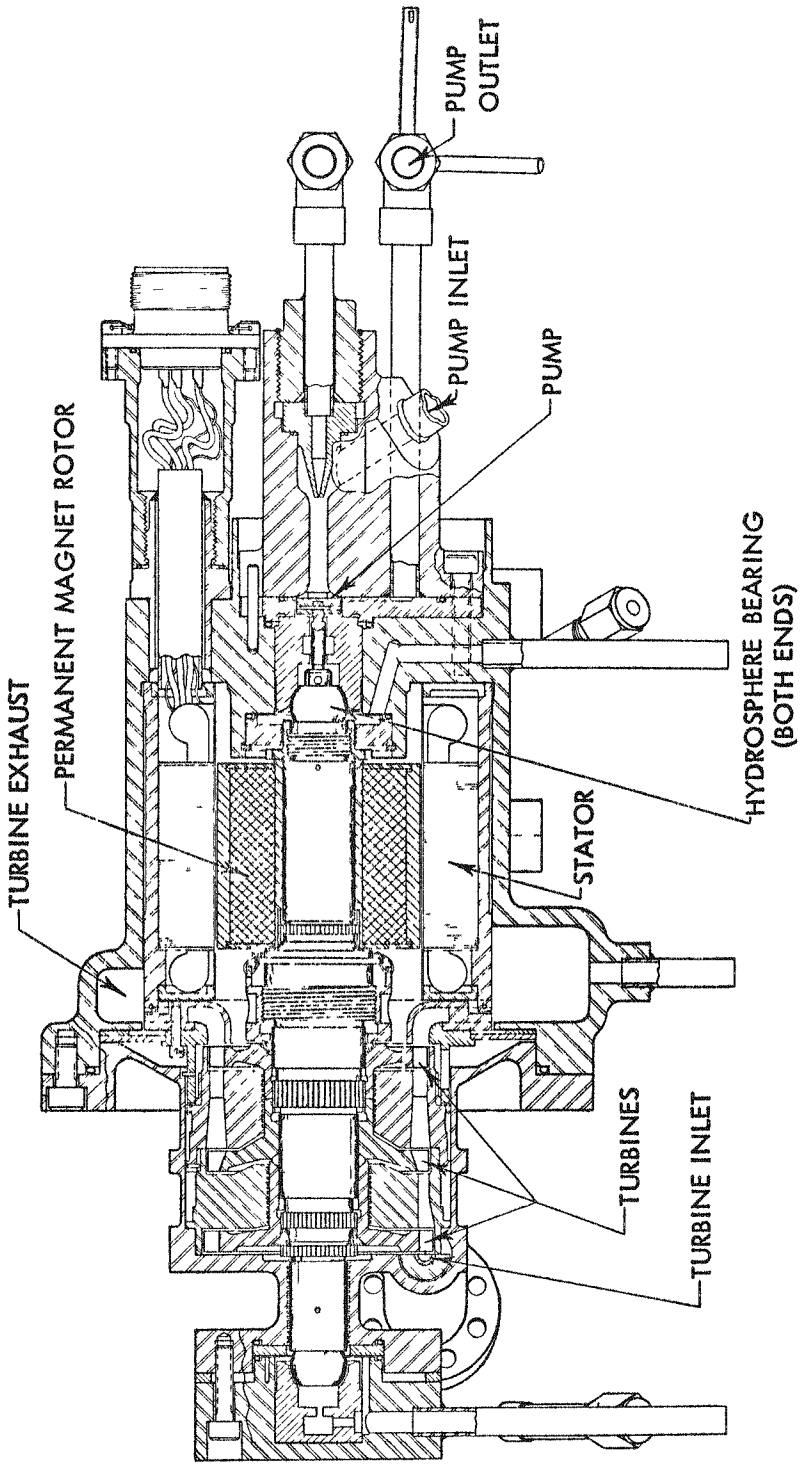

FIGURE 2-1

3.0 TURBINE SPECIFICATIONS AND REQUIREMENTS

The turbine for the SNAP I power conversion system was required to supply sufficient power to drive the alternator and pump at the design speed and to overcome the parasitic losses of the unit. Additional considerations were no external leakage and a minimum weight. The specific design objectives of the turbine varied as the SNAP I power output requirements were increased and the system design was formulated. This over-all system development resulted in the final turbine design requirements listed below:

SNAP I Turbine Design Specifications

Fluid	Mercury Vapor
Shaft Speed, RPM	40,000
Inlet Total Pressure, psia	210
Inlet Total Temperature, °F	1300
Exhaust Pressure, psia	2.06
Weight Flow, lbs/sec	.0311
Power output, watts	654
Efficiency, percent	40.0
Life, days	60

Due to the required low power output, and operation at a high pressure ratio with mercury vapor working fluid, the turbine for this application had to be a specialized design. A discussion of the turbine design considerations is included below.

3.1 Reliability

Reliability was a prime design consideration since the turbine was required to operate continuously and unattended for at least 60 days. This criterion emphasized the need for the selection of a design resistant to wear, fatigue, erosion, or seizing.

3.2 Weight

The weight of the turbine had to be a minimum because of the SNAP I orbital mission. A heavier design could have been accepted only if a greater degree of reliability or performance were obtained.

3.3 Efficiency

The attainment of optimum turbine efficiency was an important design consideration since turbine efficiency directly influenced the over-all system efficiency.

3.4 Erosion

Erosion is detrimental to satisfactory turbine operation, since it may impair reliability, cause physical damage, and reduce efficiency. Considerable care had to be exercised to reduce erosion effects to a minimum and maintain performance and reliability at a high level.

3.5 External Leakage

Leakage from the closed system could not be tolerated. The use of a make-up feed system imposed a high weight penalty and limited the life of the system. Consequently, zero external leakage was imposed as a necessary design specification.

3.6 System Integration

The effect of the turbine configuration and characteristics on the system had to be evaluated and matched with the characteristics of the other components in order to provide a compatible turbomachinery package. Specific areas of evaluation were:

a. Thermal gradients in the system package.
b. Axial and radial loads resulting from the turbine.
c. Fabrication and assembly of turbine parts in the system package.
d. Internal leakage paths in the system package.
e. Off-design turbine performance

4.0 TURBINE DESIGN AND SELECTION

The selection of a particular turbine to perform a given task at maximum efficiency requires that a comparison criteria be established which is general for all types of turbines. Thus, the best possible turbine for the objective desired will be utilized.

4.1 Turbine Parameters

Since it is rarely possible to utilize the kinetic energy of the fluid leaving the turbine, the figure of merit employed to evaluate turbine performance is the "total to static" efficiency, η_T. This is defined as the ratio of the turbine aerodynamic work output per unit mass of fluid to the work obtainable in an isentropic expansion from nozzle inlet total pressure to exhaust static pressure. This theoretically obtainable work per unit mass may be expressed as $C_{th}^2/2g$ where C_{th} is called the equivalent velocity of the available energy.

A useful guide to turbine design selection is obtained by plotting the turbine efficiency versus the ratio of rotor blade tangential speed to the isentropic velocity, (u/C_{th}), for various types of turbines (see Figure 4-1). It can be seen that different types of turbines have their maximum performance at various u/C_{th} ratios. The regenerative, Curtis, and partial admission axial flow turbines reach their peak at low values while full admission axial flow impulse turbines operate most efficiently at a value of approximately .5.

The specific speed parameter is also significant in defining the general type of turbomachinery because different classes of machines have their maximum efficiency within a relatively restricted range of specific speed. The specific speed, N_s, is given by:

$$N_s = \frac{\text{rotational speed (volume flow rate)}^{1/2}}{(\text{head})^{3/4}}$$

A plot of efficiency vs specific speed, as shown on Figure 4-2 reveals that for a low specific speed application low efficiencies are expected. This point is significant because the low power output and high pressure ratio of the SNAP I turbine implies low specific speed machinery. The low efficiencies experienced with low specific speed turbomachinery are a result of the increased effect of certain types of losses as shown in Figure 4-3.

The shaft output power of the SNAP I turbine is determined by the input power to the alternator plus the summation of the component powers of the mercury pump, mercury lubricated bearings, and the power losses resulting from windage in the package.

The experimental turbine efficiency, η_t, is expressed as;

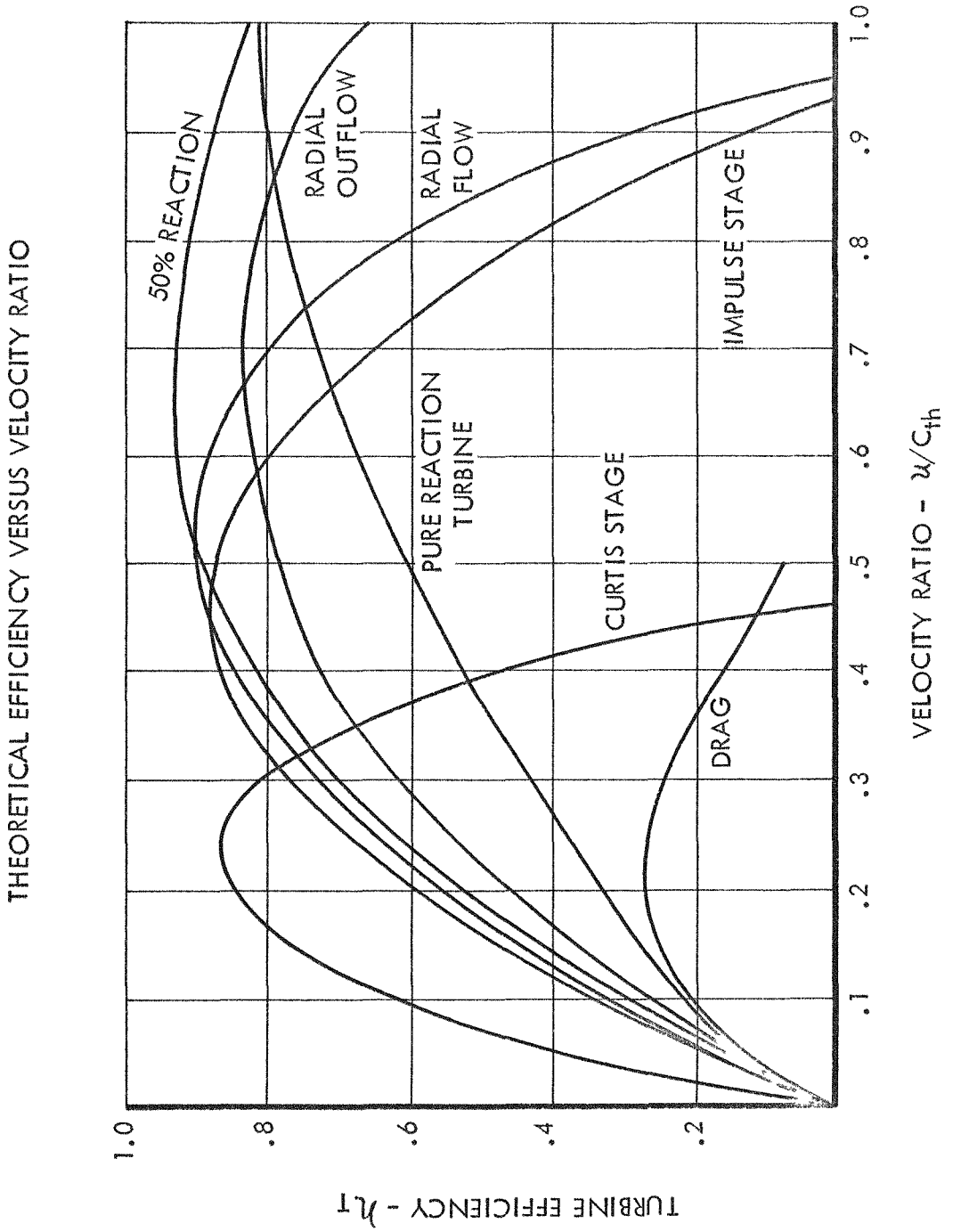
THEORETICAL EFFICIENCY VERSUS VELOCITY RATIO
50% REACTION
RADIAL OUTFLOW
RADIAL FLOW
PURE REACTION TURBINE
CURTIS STAGE
IMPULSE STAGE
DRAG
1.0
.8
.6
.4
.2
TURBINE EFFICIENCY - η_T
.1
.2
.3
.4
.5
.6
.7
.8
.9
1.0
VELOCITY RATIO - u/C_{th}

FIGURE 4-1

EFFICIENCY AS A FUNCTION OF SPECIFIC SPEED FOR SEVERAL TURBINE TYPES

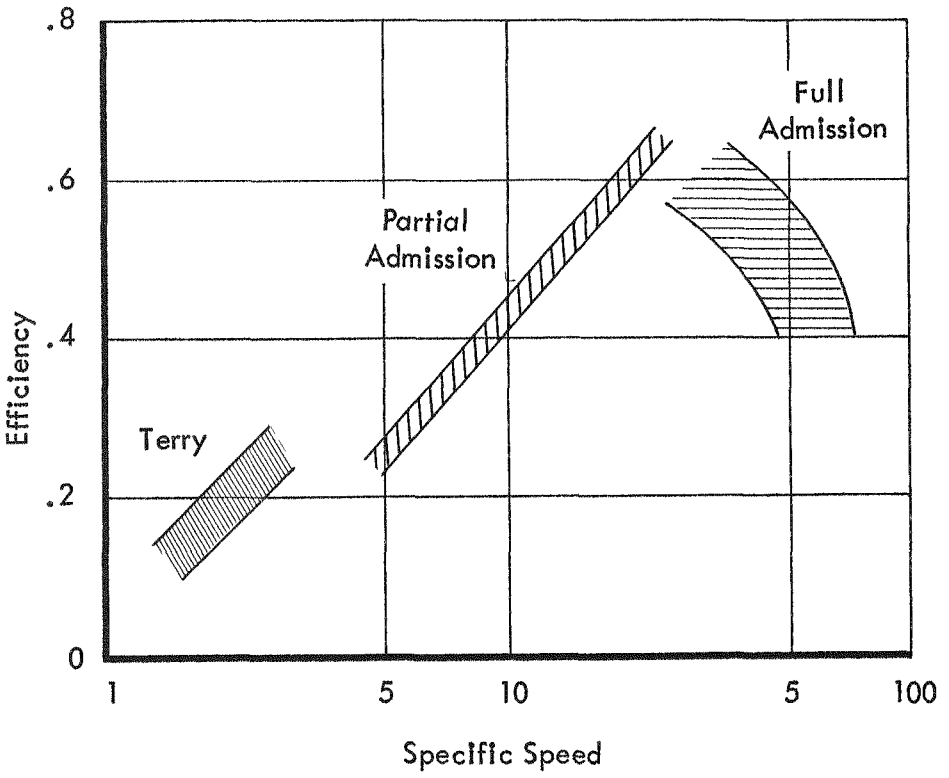

FIGURE 4-2

LOSSES VERSUS SPECIFIC SPEED

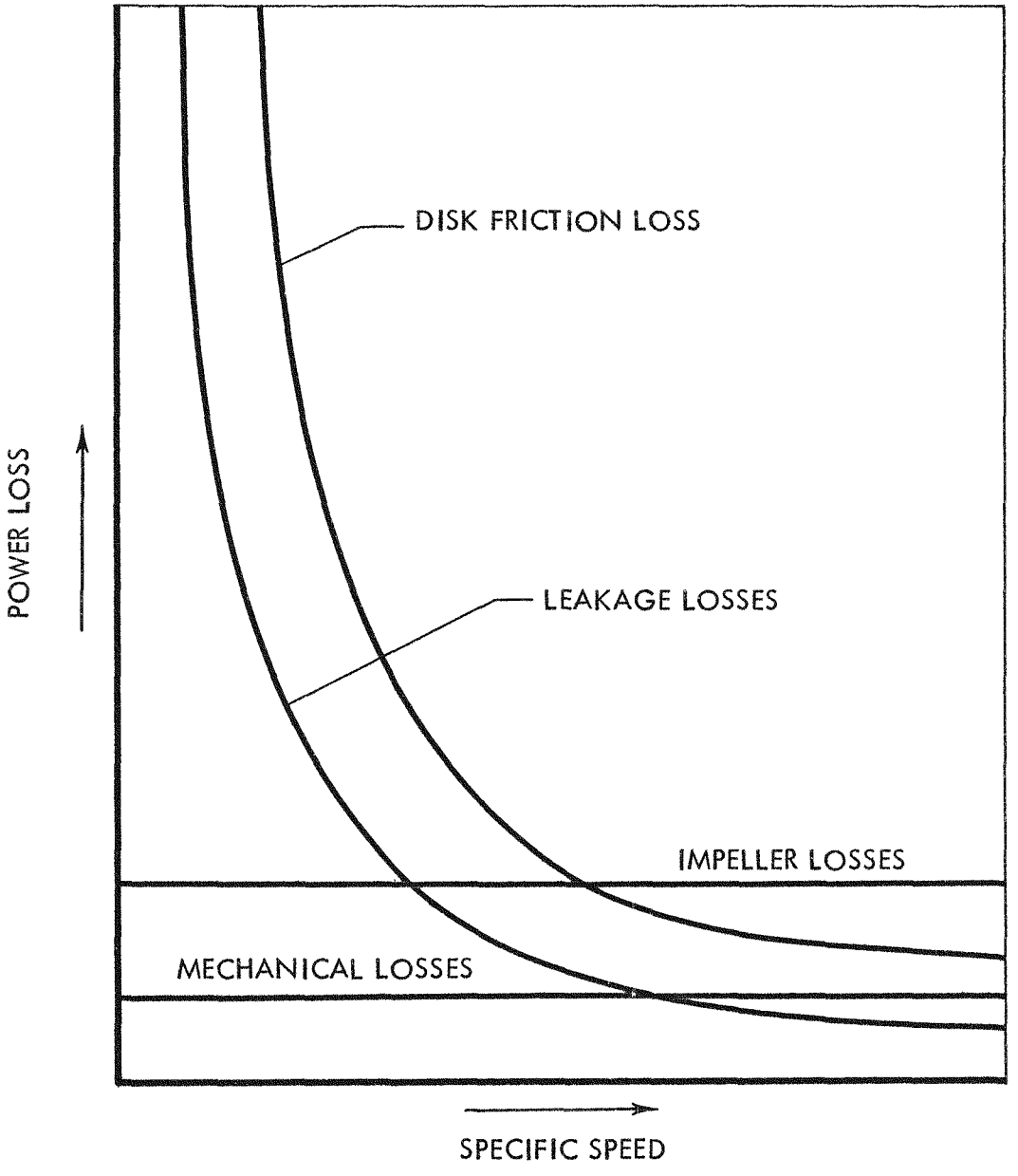

FIGURE 4-3

$$\eta_t = \frac{K_1 \text{ (turbine shaft power output)}}{W_f \ (h_{oo} - h_e)} \qquad (1)$$

Turbine total weight flow, W_f, for a choked nozzle is obtained from the relationship;

$$W_f = \frac{K_2 \quad A_t \quad P_{oo}}{\sqrt{T_{oo}}} \qquad (2)$$

where:

K_1 = Constant
K_2 = Constant
h_{oo} = Turbine inlet total enthalpy
h_e = Turbine isentropic exhaust enthalpy
η_t = experimental turbine efficiency
A_t = Nozzle throat area
P_{oo} = Nozzle inlet total pressure
T_{oo} = Nozzle inlet total temperature

4.2 Turbine Design Considerations

In the design of turbines in the power and pressure ratio ranges of the SNAP I application, quantitative information on "secondary" losses is required. For turbines developing less than 50 hp the effects of second order losses have sufficient influence to affect the selection of the basic turbine type as well as the design details.

As indicated in Figure 4-3, the fluid leakage past seals and around the ends of turbine blades becomes of sufficient magnitude to profoundly influence over-all performance of a low specific speed turbine.

As flow is reduced, an additional effect is the reduction of Reynolds' number with a corresponding increase in flow losses. The increased disc friction losses can be correlated with the change in Reynolds' number and the geometry of the turbine. In addition, as flow area is reduced, partial admission may become necessary as a result of reduction in working fluid flow area to the point where the entire periphery of the turbine cannot be utilized. Minimum turbine blade annulus area is established when the penalties associated with partial admission are less than the alternate penalties associated with reduction in turbine diameter and blade height. The losses associated with partial admission stem from two sources: Parasitic work is required to drive the unused blades through the turbine housing environment, and losses are encountered in accelerating the static fluid contained in the blade passages as they enter the active jet area.

High pressure ratio turbines require the extraction of high energy per stage if multi-staging is to be avoided. High energy extraction per stage results, generally, in high nozzle velocities and high optimum wheel speeds. If the optimum wheel speed is impractical, due to the limitations of the load or to wheel stress considerations, the turbine will not effectively extract energy from the working fluid. An additional adverse effect of high velocities is the increase in flow losses and nozzle to blade transition losses, especially with supersonic relative blade entrance velocities.

Multi-staging offers some advantages that improve turbine performance, but the price paid for additional stages in some cases nullifies the gains. Included in this price is the additional complexity and weight of a multi-staged turbine and amplification of some of the losses which have been described. The general consideration of multi-staging is clouded by the difficulty in directing a small stream of fluid through nozzle-blade-nozzle transitions without quickly losing effectiveness due to spillage, turbulence and general flow scatter.

When the working fluid is a vapor near the dewpoint, an additional problem arises from evaluation of erosion caused by the impact of high velocity droplets on turbine elements. Since over-all cycle efficiency is enhanced when the energy extraction process leaves the working fluid with the maximum moisture content, an optimum design requires accurate knowledge of the degree of supersaturation which can be utilized, and/or of the extent to which condensation can be tolerated by the materials being used.

An additional consideration in evaluating turbines for space power unit applications is the effect of turbine speed on the weight of electrical power generating equipment. By operating electrical equipment at high speed and producing high frequency power, the size and weight of this machinery is reduced considerably.

Turbine efficiency is an important system consideration because of the problem of heat rejection. Space power plants must reject all heat by radiation to space. The weight of the radiator, in even the smallest power plants, is a large fraction of the total system weight. In addition to having a great influence on radiator weight, the turbine efficiency has a considerable influence on the size of the energy source required.

4.3 Turbine Types

The following section is a discussion of the feasibility of several types of turbines for use in the SNAP I power conversion system. The types of turbines are briefly discussed by evaluating their characteristics according to the criteria established in the previous sections.

4.3.1 Pure Reaction Turbine

The pure reaction turbine is a simple radial outward flow machine and it is the first device recorded in history involving the fundamental processes used in gas turbines and jet propulsion. Vapor enters a rotor in an axial direction and escapes through tangential nozzles. Rotation occurs because of the change in momentum of the high velocity fluid leaving the nozzles. The pure reaction turbine has potential in the power ranges and sizes of interest, but extensive development would be required to obtain the high efficiency.

4.3.2 Regenerative Turbine

In the regenerative turbine, as herein discussed, the flow is in the tangential direction with repeated entry and discharge from the wheel before being discharged from the diffuser. Thus, a multi-stage effect is created with a single wheel. Types of regenerative turbines of interest include the drag turbine, a combination of internal flow drag turbine with a split-drag turbine, and a vortex turbine with redirecting surfaces for positive fluid guidance.

The regenerative turbine has definite advantages over radial or axial flow, impulse or reaction types for very small turbine applications, since it is basically a low specific speed machine and is mechanically more simple. Several regenerative turbines were evaluated at TRW since they were potentially applicable to Rankine space power systems. The initial interest was centered on the regenerative turbines in order to efficiently utilize the high pressure ratio available to the turbine and yet restrict the expansion in the nozzle to avoid erosion with condensed mercury vapor. Because of its very small effective nozzle area, this turbine is well suited to high pressure ratio, low power output applications similar to SNAP 1. Section 5.0 presents the investigations performed at TRW with this type of turbine.

4.3.3 Radial Flow Turbine

The concepts of the radial inflow and outflow turbines have been long known, but it was not until recently that they became prominent. Radial inflow turbines have been designed for low power applications with high efficiencies although the design procedures are not well established. Some advantages of the radial inflow turbine are:

a. The rotor is a simple rugged one-piece construction
b. The manufacturing costs are lower compared to multi-blade axial flow types.
c. The radial inflow turbine has a higher efficiency, (for small power outputs) compared to the axial flow type, for which the very small aspect ratio of blades and nozzles leads to a high percentage of secondary flow losses.

Some undesirable features of the radial inflow turbine are:

a. Pressure ratio limitations per stage, because of the increased specific volume of the fluid which leads to a restriction in area of the discharge.

b. Multi-staging is awkward and inefficient.

c. Excessive windage or disc friction losses.

4.3.4 Axial Flow Impulse Turbines

In axial flow impulse turbines, the entire available expansion takes place in the stators or stationary nozzles. The high velocity gases are then admitted into the rotor where the kinetic energy of the fluid is converted into mechanical energy by a change in the momentum of the working fluid. Axial flow impulse turbines have several features which are desirable for the SNAP I application:

a. Since no pressure drop occurs across the rotating part, the turbine axial thrust loads are considerably minimized. Minimum axial thrusts reduce the size of the bearings required, and hence, system parasitic power losses.

b. Leakage losses over the tip of rotating blades are reduced because of the small pressure gradient between the pressure and suction sides of the blades.

c. The state-of-the-art of impulse turbine design is well advanced.

d. Axial impulse turbines are best suited for partial entry, which is often required for small output power conversion systems.

In axial flow impulse turbines, the pressure ratio across a single stage is limited by two factors:

a. Nozzle exit velocities should not be excessive because of possible shock losses due to over and under expansion.

b. Relative approach Mach numbers to the rotors should be less than 0.85 because of possible shock losses and separation of the boundary layer from the blade surface. (However, some supersonic rotors have been successful)

Since the final SNAP I turbine was an axial flow impulse turbine, a detailed discussion of impulse turbines is included in section 6.0.

4.3.5 Axial Flow Reaction Turbine

In an axial flow reaction turbine, a portion of the pressure drop occurs in the nozzle section and the remainder in the rotating blades. For reaction type turbines the peak efficiency is less sensitive to variations of the u/c than the impulse type. The wide latitude permissible in the selection of the percentage of reaction to be employed leads to

more freedom in the selection of the other design variables than is possible with the impulse turbine. The state-of-the-art of reaction turbine development is as well advanced as that of the impulse type.

Reaction turbines differ from impulse turbines as follows:

a. There is need for close mechanical clearances between the tips of rotating blades and casing, in order to minimize leakage over the tips and consequent mixing losses as the leakage flow recombines with main stream of blade exit.

b. All blade contours give convergent channels, resulting in reduced frictional losses since a pressure gradient in the direction of the flow suppresses the boundary layer along the walls of such channels. This results in higher stage and turbine efficiencies.

c. Full admission of the vapor must exist throughout the entire periphery of the rotor in order to sustain a uniform pressure drop across the rotating blades.

d. Because of the pressure drop across the rotor, there exists an axial thrust on the shaft which must be supported by the bearings.

4.3.6 Terry Turbine (Velocity-compounded)

The Terry Turbine is a velocity-compounded turbine in which the fluid enters the wheel radially and follows a helix-like path. As the fluid leaves the first bucket, it enters a reversing bucket placed over the wheel, which returns it into the wheel. The turning angle of the fluid through the passages of a Terry type turbine rotor is 180° regardless of the inlet nozzle angle. Because of this, the Terry type turbine has been analyzed for the minimum passage angle that is practical to machine or cast. Results of the analysis for small turbines indicate that the internal efficiency approaches a maximum of 21% for two passes through the wheel and slightly less for three passes. Previous experience on applications utilizing small Terry turbines, with a high inlet Mach number, indicates that high losses are incurred in the first pass. Therefore, the possibility of obtaining an efficiency greater than 20-23% seems rather remote.

4.3.7 Other Turbines

The axial re-entry impulse (Curtis) turbine is a velocity-compounded turbine in which the entire pressure drop occurs in the nozzle and velocity decreases during passage through the moving blades. Design point internal efficiencies of a single wheel impulse turbine utilizing two and three passes of the working fluid through the blades indicate that a slight gain in efficiency can be realized by a third pass. The re-entry impulse turbine reduces partial admission losses but adds problems in fabrication and turning losses. An alternate arrangement of the re-entry turbine is the cantilevered blade, radial flow turbine. This

type of turbine has less turning loss in the first re-entry passage than does the axial re-entry turbine. The reduced losses reflect an increase in efficiency over the 3 pass axial re-entry. In addition, this arrangement reduces the fabrication difficulties of the 3 pass axial re-entry configuration.

4.4 Turbine Selection

The preceding discussion has indicated the advantages and problem areas of the different turbines applicable to SNAP 1. The regenerative turbine was selected for the early Rankine space power turbine feasibility investigation program in order to obtain a more thorough understanding of the loss phenomena of these small turbines. A discussion of the regenerative turbine development is included in Section 5.0.

During this early turbine program, a more thorough analysis of the axial flow turbine was undertaken and indicated that it had definite advantages for use in SNAP 1. Preliminary tests using air verified the analysis and effort was directed to the three stage axial flow mercury vapor turbine as discussed in Section 6.0.

5.0 REGENERATIVE TURBINE DEVELOPMENT

The turbine experimental development program was established to determine feasibility, correlate analytical and experimental results, and develop a turbine capable of meeting the requirements of Rankine space powerplants. This required analytical and experimental investigation of low power output, high pressure ratio, high speed, reliable mercury vapor turbines.

The turbine experimental program consisted of tests of variations of the regenerative type turbines (steam drag turbine, air drag turbine, and air vortex turbine), and the air axial flow single stage impulse turbine which was designed to simulate one stage of a three stage axial flow mercury vapor turbine. A brief discussion of the component development history of the regenerative type turbines is included in this section of the report.

5.1 Regenerative Turbine Analysis

The regenerative turbine, as herein discussed, is a turbine in which the flow is in the tangential direction with repeated entry into the wheel. The types of regenerative turbines which were investigated analytically and experimentally were the drag turbine and the vortex turbine.

A schematic flow pattern in a drag turbine is shown in Figure 5-1. The mechanism of energy exchange between the working fluid and the drag turbine wheel is described in the following manner. The fluid, after entering the inlet port and expanding through a nozzle, enters the blade passage where a change of angular momentum takes place. The flow then proceeds around the periphery in a helical path, regaining absolute velocity after each pass through the blade passages by virtue of a pressure drop in the mean direction of flow. Flow into the moving blade passages is then the result of a radial gradient produced by centrifugal body forces acting on the fluid in the scroll. Consequently, a multistage effect is obtained before the fluid is discharged at the outlet port, which is sealed from the intake port by a stripper seal.

To utilize the high thermal efficiencies of the mercury Rankine cycle, it is necessary to employ high pressure ratios across the turbine. Conventional single stage turbines exhibit poor efficiency for high pressure ratios and multistaging is therefore necessary. The regenerative turbine has the feature of providing this multistage effect by multiple entry of the flow around the periphery of a single wheel.

The regenerative turbine has other potential advantages for very small turbine applications, since it is basically a low specific speed machine and is mechanically more simple than other turbine types. Moisture associated with the nozzle expansion in a conventional turbine does not occur in the regenerative type, since the major portion of the pressure drop occurs as the flow passes around the wheel with frictional reheating keeping the vapors dry. A moisture separating feature is also inherent in the regenerative turbine by centrifugal separation. This feature potentially allows the regenerative turbine to operate with substantially less superheat than conventional turbines. Higher turbine efficiency can

SCHEMATIC FLOW PATTERN IN A DRAG TURBINE

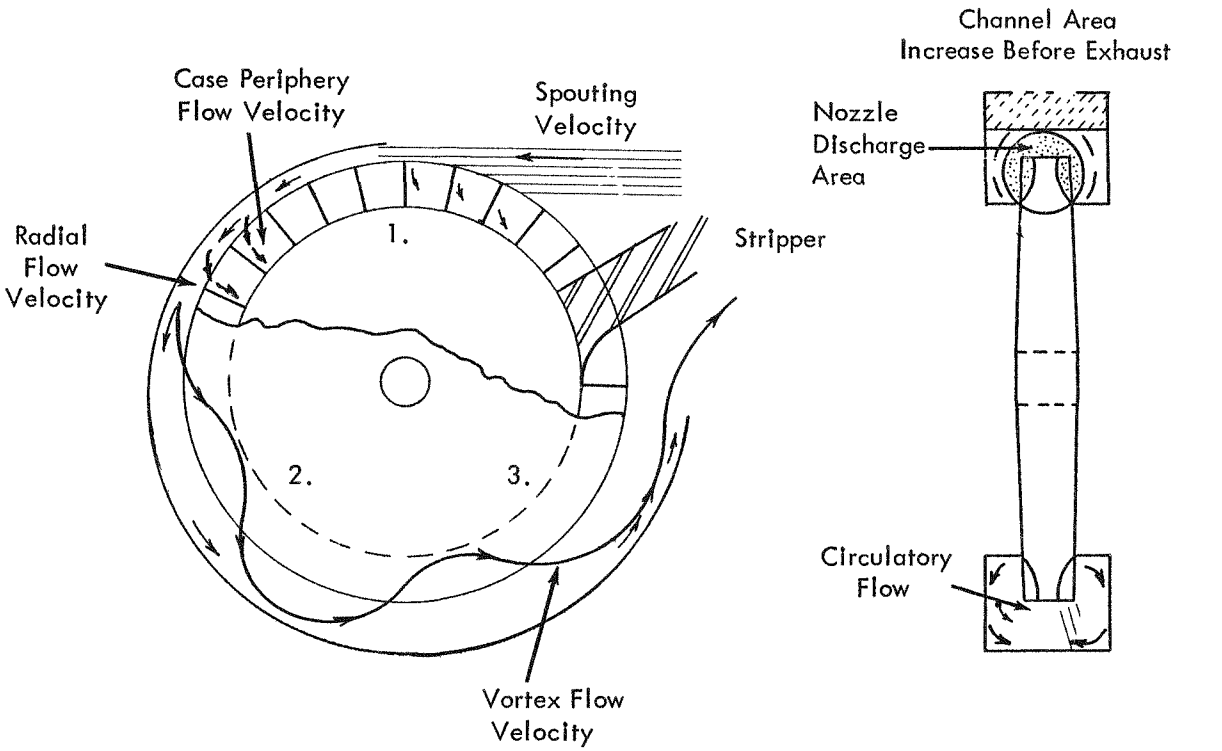

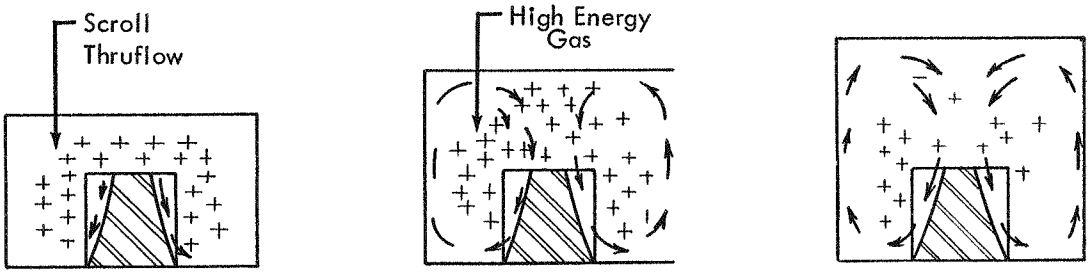

1.	2.	3.
Beginning of Circulatory Flow	Completion of One Spiral Path	Charge of Moment of Momentum in each Helinal Swirl

FIGURE 5-1

also be utilized with less concern over erosion damage.

Some of the apparent problem areas in the drag turbine are the unpredictable flow pattern through the turbine, the losses associated with the high velocity exhaust fluid, the losses due to the sudden expansion at the nozzle exit, and the losses due to fluid expansion in a constantly enlarging channel where the blade path area becomes a small proportion of the total flow area. The peripheral pressure distribution in the drag turbine scroll exerts an unbalanced radial load on the rotor which must be supported by the bearings.

A major consideration in the energy transfer between a fluid and a rotor involves the ramifications of turning the residual blade velocities of the fluid and efficiently controlling its momentum for re-entry. From the schematic it is observed that the fluid follows a vortex or helical flow path through the turbine. This vortex flow path is set up by the blade pressure gradient, angle of entering gases, and the curvature of the flow passages. Some indications of the streamlines have been found in drag pump tests from which a theoretical analysis on a two dimensional basis has been developed in terms of geometry and drag factors, as well as other flow parameters involving several variables.

An analytical investigation of the vortex and drag turbines was conducted in order to formulate general equations for the design and experimental evaluation of these turbines. The analysis was performed by setting up the basic momentum, energy, and continuity equations; combining these equations into a general equation for this type of turbine, and substantiating the general equations with existing experimental test data on the vortex and drag turbines.

The general correlation of the experimental data with theory indicated that the equations developed for these turbines approximately describe the actual dynamics in the rotor. From the correlation of the analytical and experimental results, the following conclusions were drawn:

1. The drag turbine wheel has relatively low efficiencies (approximately 15-20%).

2. The vortex turbine wheel has capabilities for higher efficiencies (approximately 30-40%).

3. When using a high temperature fluid, heat losses from the turbine casing can become significant compared to power output, a characteristic common to small turbines.

4. Drag and vortex turbine efficiencies may be reasonably estimated by the derived analytical equations.

5.2 Steam Drag Turbine Tests

Preliminary testing of the drag turbine was accomplished with steam as the working fluid. It was believed that the familiarity with and the solution of the problems associated with water vapor would expedite the later solution of similar problems with mercury vapor. Figure 5-2 is a photograph of the experimental drag turbine showing the wheel and housing. This wheel was obtained from a drag pump for preliminary turbine experimental evaluation. The inlet nozzle, turbine scroll, and exhaust diffuser were designed and fabricated to incorporate the drag wheel. Testing of the drag turbine with steam as the working medium was completed under the following conditions of operation:

1. Nozzle inlet total temperatures: up to 330°F
2. Nozzle inlet total pressures: 32 to 90 psia
3. Steam mass flows: 318 to 878 lb/hr
4. Turbine speeds: 13,500 to 52,000 rpm
5. Turbine power outputs: 388 to 2220 watts

The following test results were obtained:

1. Satisfactory operation of an aluminum wheel with saturated steam impinging on the blades at relative velocities up to 2300 ft per sec showed negligible evidence of blade damage or erosion.

2. Turbine efficiencies varying from 8 to 22% were obtained for u/c_{th} ratios of .10 to .28 with preliminary blade and scroll aerodynamic profiles.

3. Reasonably quiet and vibrationless operation was observed.

4. Flow paths around the drag turbine periphery were obtained by white lead "paint picture tests" and showed the existence of secondary flows in the scroll.

5. Static pressure measurements around the scroll indicated the feasibility of providing operation with reaction even for very low power outputs.

A curve of turbine efficiency versus u/c_{th} for various total pressure ratios is shown in Figure 5-3. This curve shows that the efficiency reached a maximum at a u/c_{th} value of approximately .25.

The variation of the static pressure along the mean flow path through the turbine and diffuser may be found in Figure 5-4. It is seen that energy extraction from the steam is obtained around the turbine scroll with the majority of energy extraction in the first 180°. The curve shows that the efficiency was lowered considerably by the losses due to the pressure drop around the 90° bend at the turbine outlet and the poor performance of the subsonic diffuser. These losses increased with increasing mass flows. For the maximum

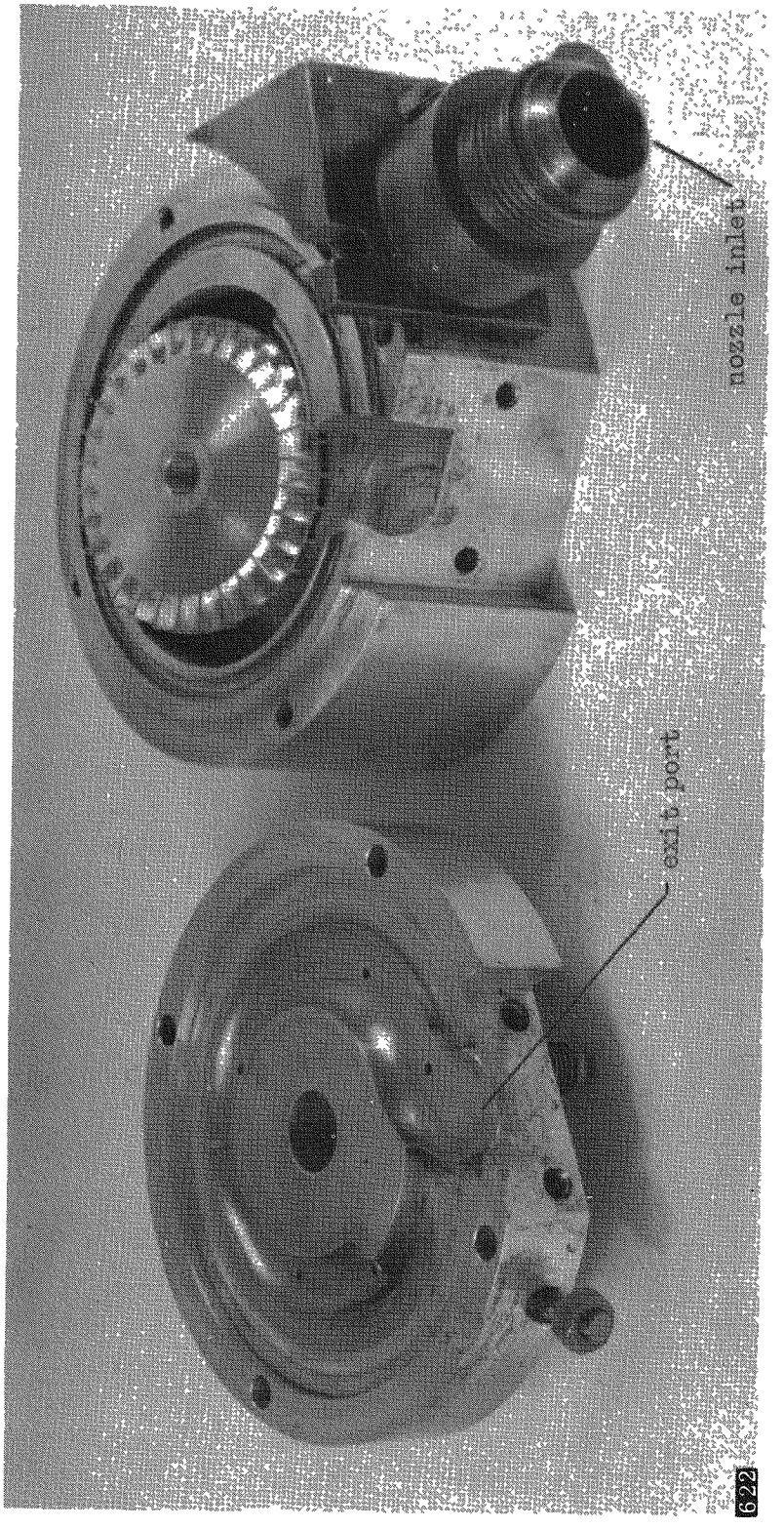

EXPERIMENTAL DRAG TURBINE

FIGURE 5-2

STEAM DRAG TURBINE EFFICIENCY
VERSUS VELOCITY RATIO

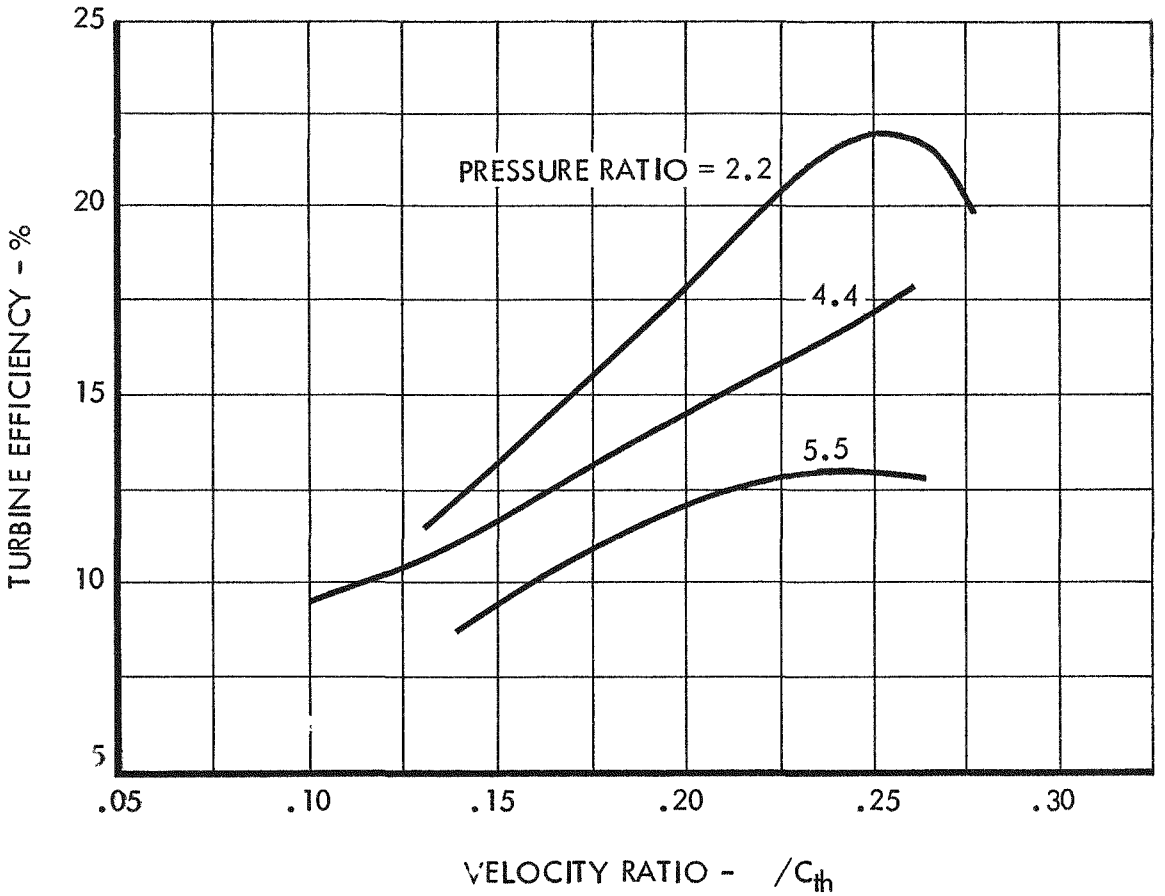

FIGURE 5-3

STEAM DRAG TURBINE PRESSURE VS. MEAN FLOW PATH THROUGH TURBINE AND DIFFUSER

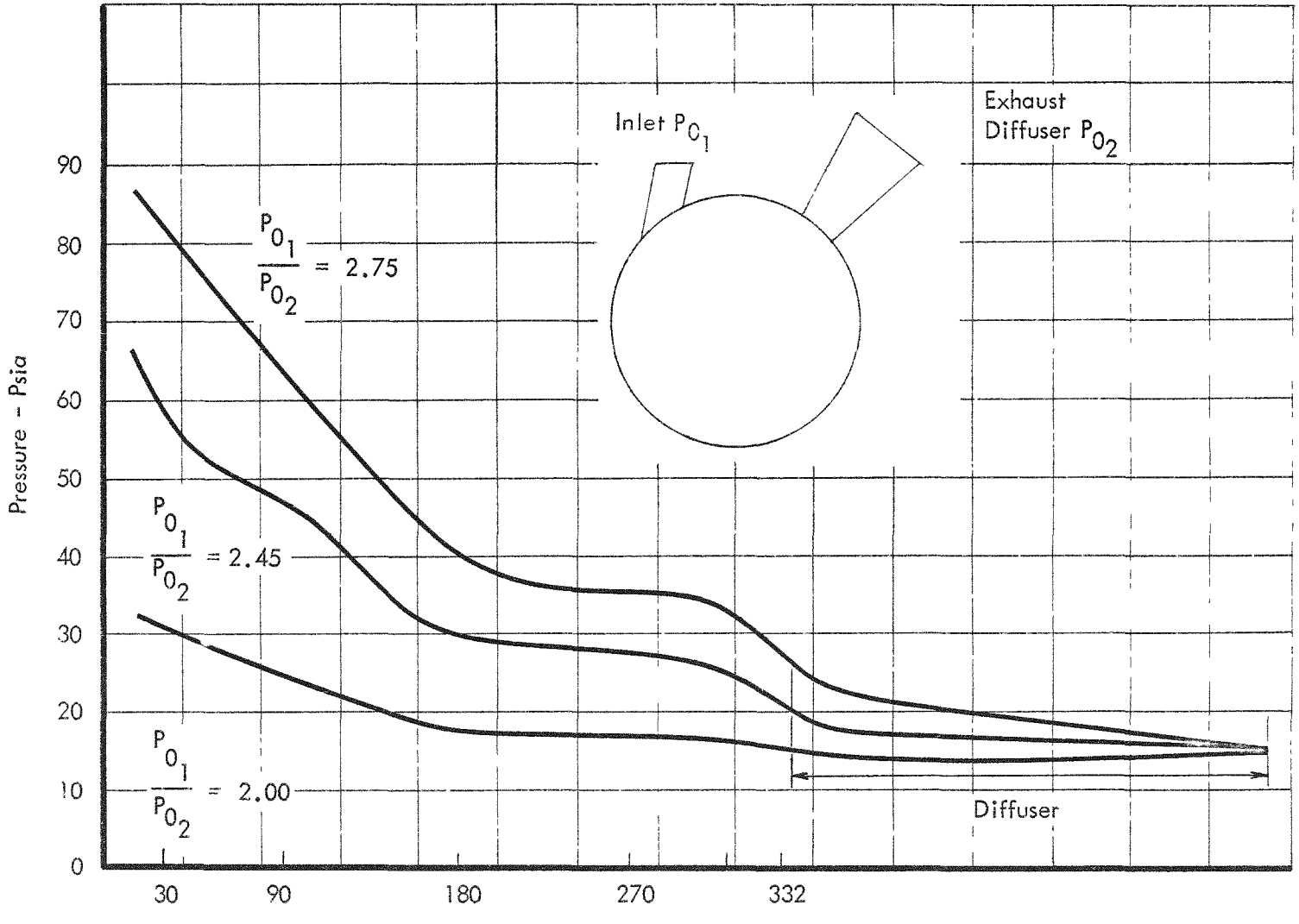

FIGURE 5-4

flow rate, a pressure drop of 12 psi was encountered around the 90° bend and static pressure loss was observed in the diffuser. The overall turbine efficiency is improved appreciably by reducing the high velocity bend and incorporating a revised exhaust diffuser to minimize the pressure losses in the turbine exhaust. This would approximately double the rotor pressure ratio.

Success of the regenerative turbine in reducing the nozzle pressure ratio may also be seen from Figure 5-4 which shows that the nozzle operated subsonically throughout the range of pressures encountered in these tests.

Power outputs up to 2200 watts were obtained with the steam drag turbine at speeds up to 45,000 rpm at various total pressure ratios. These tests were run with relatively low pressure ratios across the turbine rotor due to the high losses in the exhaust stack from the rotational components of the exhaust flow velocity.

The steam drag turbine tests showed realistic turbine efficiencies of approximately 22% and indicated that these efficiencies could be improved by further redesign and development.

5.3 Air Drag Turbine Tests

Due to the low pressure ratios available for operation with steam and the availability of a high pressure air supply (225 psia), it was decided to use air for further turbine type feasibility testing. Pressure ratios of 15 to 1 could be obtained with the existing laboratory air facilities, whereas the addition of a condenser or ejector to increase the pressure ratio with steam involved unwarranted costs and complications.

The drag turbine wheel and housing used in the steam tests were utilized for the air drag turbine tests and were operated under the following conditions:

1. Nozzle inlet total temperatures: up to 70°F
2. Nozzle inlet total pressures: 44 to 140 psia
3. Air mass flows: 700 to 2400 lb/hr
4. Turbine speeds: 15,700 to 47,000 rpm
5. Turbine power outputs: 500 to 2400 watts

Air drag turbine test results indicated substantially the same results as the steam drag turbine tests, except for the following:

1. Lower efficiencies were indicated with air than with steam.
2. Air drag turbine efficiencies varied from 7 to 13% over a range of u/C_{th} of .12 to .31.

A curve of the air drag turbine efficiencies versus the u/C_{th} ratio for various total pressure ratios may be found in Figure 5-5.

AIR DRAG TURBINE EFFICIENCY
VERSUS VELOCITY RATIO

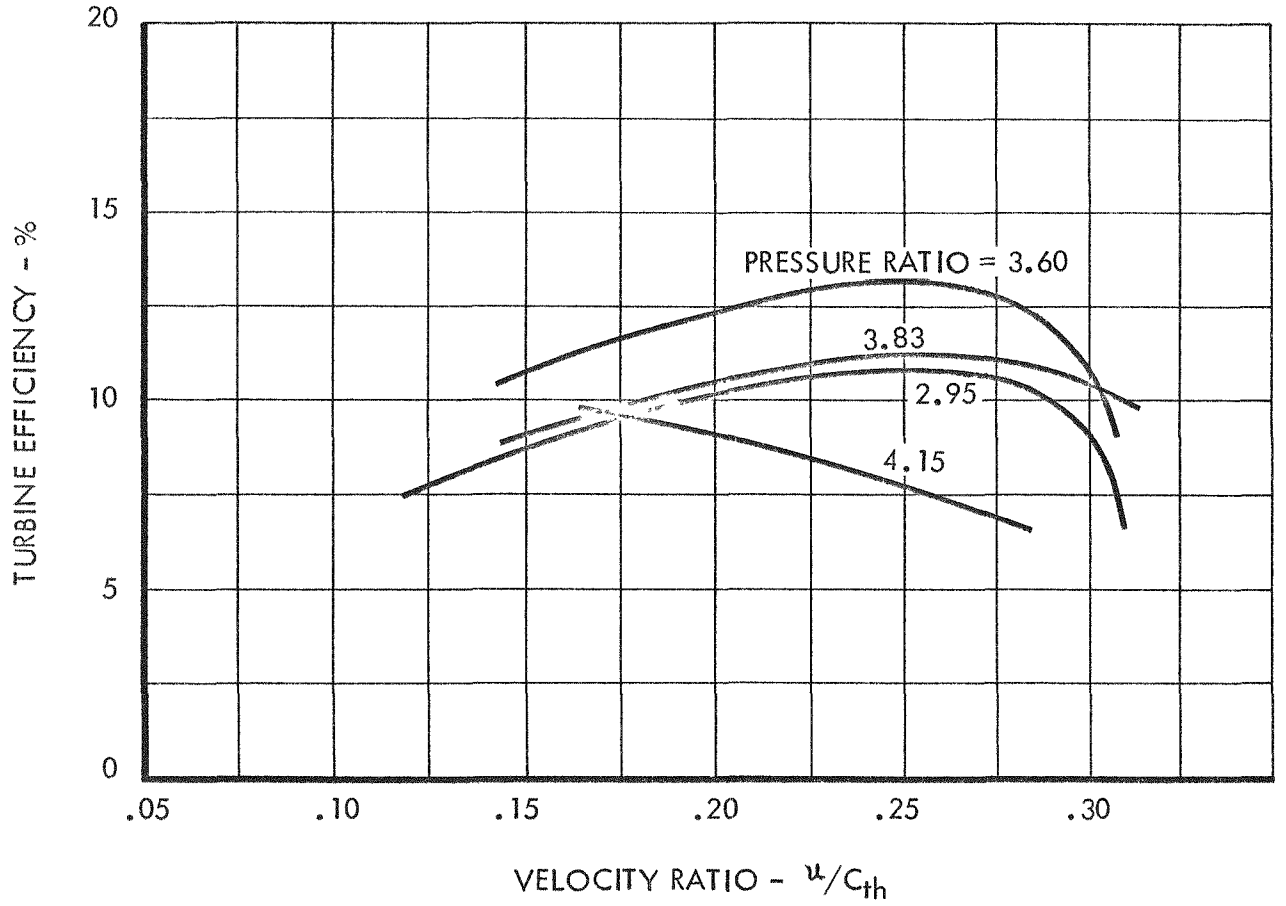

FIGURE 5-5

The nozzle operated in the subsonic flow range throughout the range of pressures encountered in these tests. Energy extraction from the air was obtained around the turbine scroll with the majority of energy extraction in the first 180°.

5.4 Air Vortex Turbine Tests

Since relatively low efficiencies were obtained with the air and steam drag turbines, an investigation of the analytical and experimental drag turbine results was conducted to determine an improved regenerative turbine design. An analysis of the paint picture tests of the drag turbine revealed the existence of strong secondary flows in the scroll. The fundamental cause of these secondary flows could be eliminated by changing the bacic concept of the drag wheel geometry to that employed by the vortex turbine. Consequently, a vortex turbine was designed which incorporated features based on the previous experience with drag turbine tests.

A photograph of the vortex turbine, Figure 5-6, shows the turbine wheel, nozzle, housing, and fan for the air absorption dynamometer. The vortex turbine wheel was approximately 2-3/4 inches in diameter and 5/8 inches wide with labyrinth seal grooves on the sides of the wheel. The first turbine scroll design did not utilize re-entry vanes and attained a maximum turbine efficiency of 21%. In an attempt to improve the initial vortex turbine performance, several variations of re-entry vanes were incorporated in the scroll of the housing to provide positive guidance of the fluid.

The performance characteristics of the vortex turbine with the smooth scroll and with the re-entry modifications are shown in Figure 5-7. The efficiency decreased considerably with the addition of the re-entry vanes in the turbine scroll to provide positive fluid guidance, and the high pressure vane re-entry provided more severe losses than the low pressure vane re-entry.

Nonuniform flow was observed at the vortex turbine exhaust by traversing the diffuser flow path with a total-static pressure probe. The results of the traverse indicated approximately half of the diffuser had a negligible flow velocity, indicating separation in the diffuser.

Vortex turbine efficiency could be increased appreciably by redesign and development of the nozzle and diffuser. Calculations of the vortex turbine rotor efficiency indicated a maximum efficiency of 32% as computed by dividing the measured enthalpy decrease across the rotor by the ideal enthalpy drop as determined from the rotor pressure ratio. This assumes that the nozzle and diffuser are not part of the turbine, which is justifiable if primary interest is in the rotor dynamics and verification of theory and experiment. This is based on the concept that the nozzle produces the through flow velocity and the diffuser recovers this velocity.

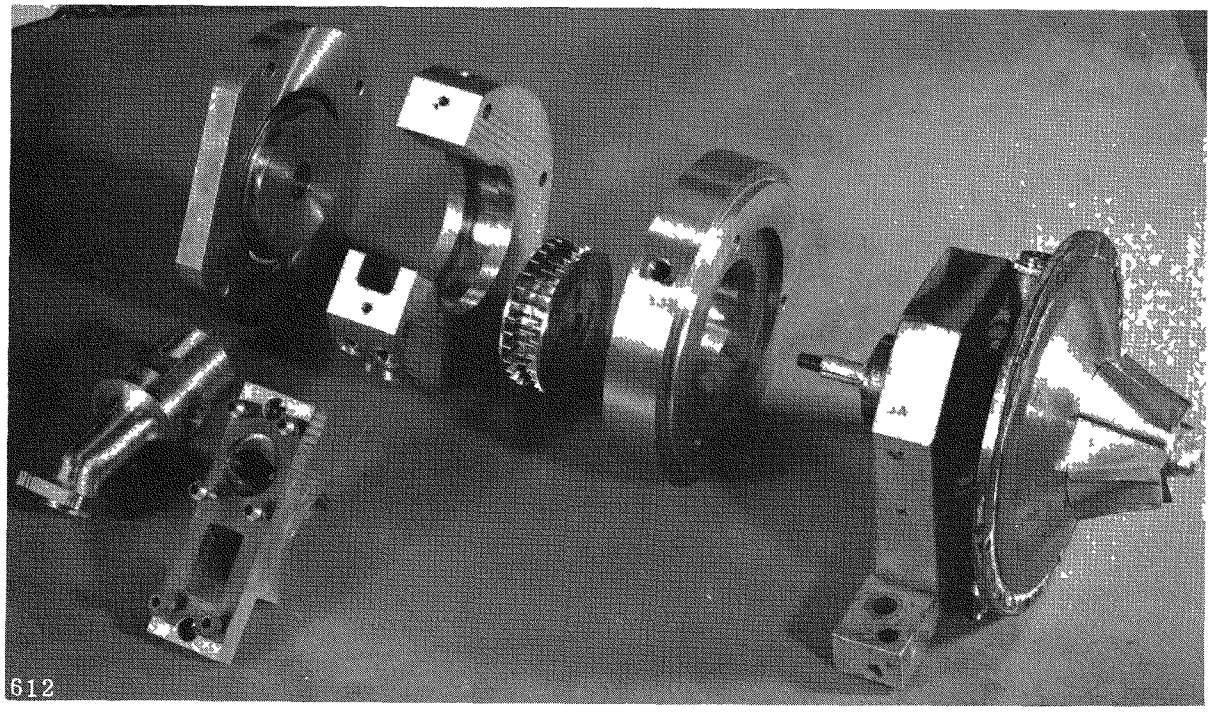

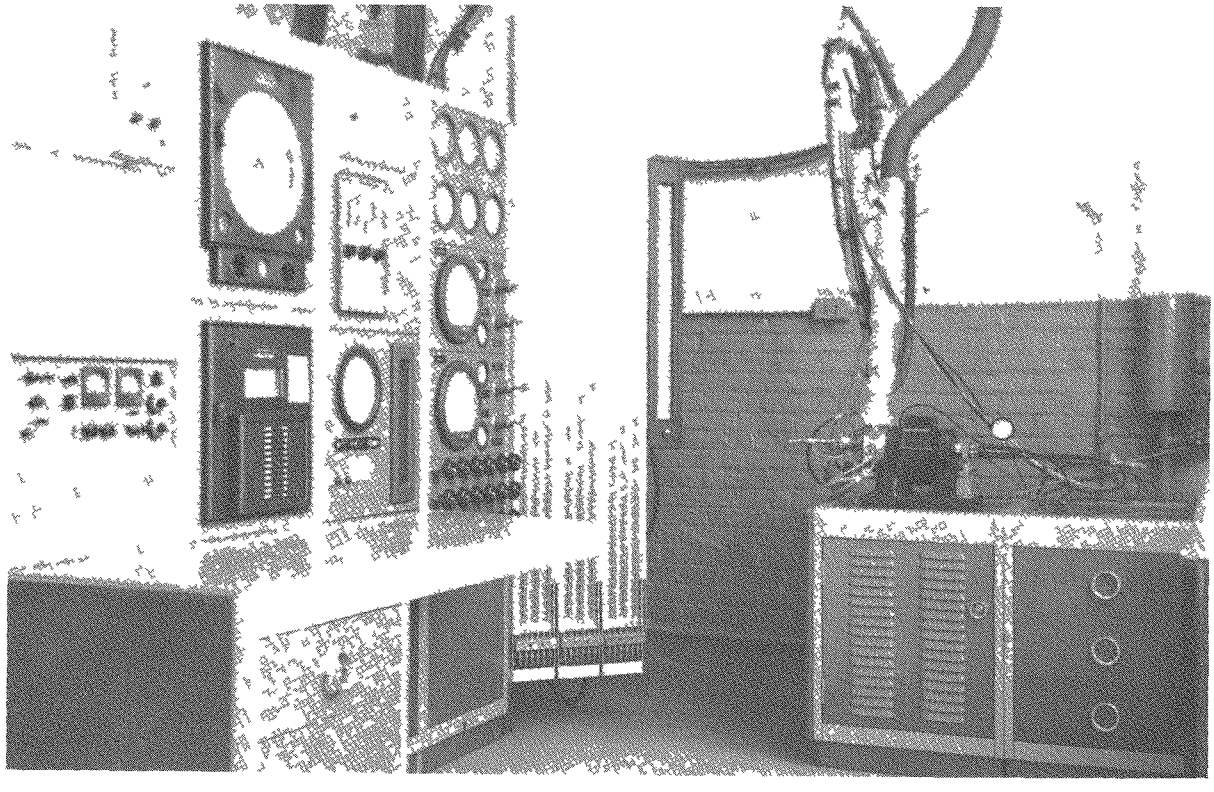

AIR TURBINE DYNAMOMETER WITH INSERT SHOWING VORTEX TURBINE AND TURBINE DYNAMOMETER

FIGURE 5-6

PERFORMANCE CHARACTERISTICS OF
VORTEX REENTRY TURBINE

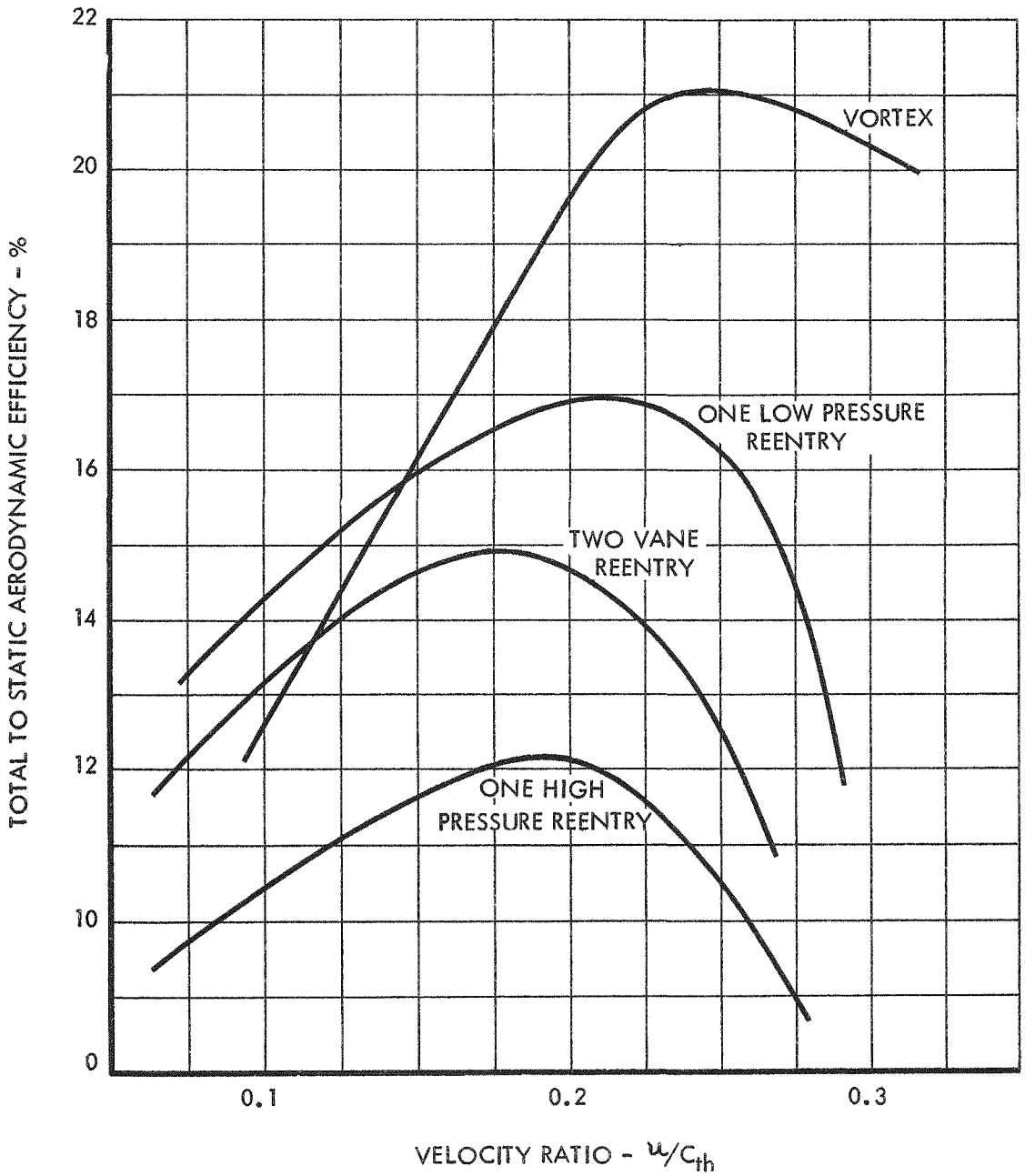

FIGURE 5-7

6.0 THREE-STAGE AXIAL FLOW TURBINE DEVELOPMENT

Analytical and experimental investigation of the regenerative-type turbines (steam drag, air drag, and air vortex) indicated that these turbines were relatively low efficiency machines (15-30%), and that extensive analytical and experimental development would be required to obtain a turbine efficiency of 40% at the SNAP I design operating conditions.

Due to the advanced state-of-the-art of axial flow impulse turbines, including advances in the analysis of partial admission losses, an axial flow impulse turbine was selected for further development to meet the SNAP I design specifications.

Preliminary tests in the air turbine test rig conducted with an axial flow single stage impulse turbine to simulate one stage of a three-stage axial flow mercury vapor turbine indicated that improved performance could be obtained with the axial flow impulse turbine over the regenerative type turbines for the SNAP I application. A three-stage mercury vapor axial flow turbine was designed and incorporated in the initial system test package. Due to the encouraging results obtained in the initial system tests, the three-stage mercury vapor axial flow turbine was incorporated in all system test packages.

This discussion is concerned with the design and experimental test results of the SNAP I three-stage mercury vapor axial flow turbine.

6.1 Axial Flow Turbine Design

Successful performance of the air impulse axial flow turbine resulted in the selection of this type of turbine for SNAP I. Performance and design calculations for the turbine of the first system test package, the Turbine-Alternator Test Package, were completed long-hand. Because of the considerable time involved in completing these calculations, only one design point was investigated. The realization that other design points should be investigated to formulate an optimum turbine design intensified interest in a computer program to calculate the turbine parameters. The abundance of literature together with the relatively advanced state-of-the-art of axial flow turbines made the computer program even more attractive. Therefore, it was decided to proceed on a turbine design program and turbine off-design program utilizing the IBM 650 digital computer. These programs, financed by Thompson Ramo Wooldridge funds, were completed in time for use in the latter portion of the SNAP I three-stage axial flow turbine development.

6.1.1 Turbine Design Program

The method used to design the axial flow turbine can be generally termed the "Loss Equation System." These equations were incorporated in an IBM 650 computer program to design full or partial admission, impulse or reaction, single or multi-stage, axial flow turbines. The equations included in the program account for the following losses in efficiency:

1. Heat transfer from nozzle and rotor blades.

2. Leakage through nozzle labyrinth seals and over rotor blade tips or shrouds.

3. Mixing and reheating at rotor and stator exits.

4. Incidence at the nozzle and rotor inlet caused by a mismatch of the inlet foil angles and gas angles.

5. Rotor approach Mach number.

6. Overexpansion and/or underexpansion of converging-diverging nozzles or converging straight back nozzles.

7. Rotor disc friction.

8. Reynolds number corrections.

9. Profile, turning, and aspect ratio in nozzles and rotors.

10. Pumping and mixing due to partial admission.

Expressions for these losses were based upon past experience and were derived analytically and/or empirically.

In brief, the design selection of an axial flow turbine utilizing the computer program is as follows:

An initial sizing of the turbine is accomplished longhand and depends largely upon the number of stages, and the specified cycle conditions, which determine pressure ratio, weight flow and inlet and exhaust conditions. In many instances it is not possible to select the optimum number of stages due to size or cost limitations. During the preliminary sizing, particular attention is paid to blade height to diameter ratio and aspect ratio since these two usually determine whether or not the turbine utilizes full or partial admission. In some cases, the choice between a full or partial admission turbine was uncertain and only a thorough analytical investigation resulted in the correct selection.

With the initial sizing completed, the input data to the computer was prepared. This data included the cycle conditions, axial chords of nozzle and rotor blades, mean diameter of the nozzle and rotor passages and a starting blade height for the first stage nozzle exit. The pressure distribution throughout the turbine was selected at the discretion of the designer. The computer matched the remaining geometry to the conditions originally assumed, and also determined the turbine performance.

Due to the high speed of the computer, many turbine configurations could be evaluated in a relatively short period of time and it was also possible to experiment with some unorthodox selections.

The final turbine design was selected to have its maximum performance at the design point.

6.1.2 Turbine Off-Design Program

A very useful tool for turbine performance evaluation was the IBM 650 Turbine Off-Design Program developed by TRW. This program was similar in operation to the turbine design program with the exception that all the geometry or other pertinent parameters were given as inputs and the turbine performance determined for other controllable variables such as speed, inlet or exhaust conditions, or changes in geometry.

The off-design program required more time, however, since many of the variables were not independent and had to be matched before a solution was obtained. This was done by checking continuity of flow throughout the turbine with the results obtained from the general energy equation and the "Loss Equation System", or from experimental data. The losses of the turbine are calculated by the same "loss equation system" as previously mentioned in the turbine design program. Due to the complexity of the program, only one stage at a time can be calculated.

The results of the analysis indicate the discrepancies between calculated and experimental results and the appropriate modifications that must be incorporated to reduce these discrepancies. In this way, an off-design performance trend may be established for varying speed, inlet conditions, or any other desired controllable variable.

6.2 TATP Turbine

The first SNAP I system package was the Turbine-Alternator Test Package (TATP) and was used to evaluate turbine performance. The TATP turbine was a three-stage, axial flow, mercury vapor, impulse turbine with a mean diameter of 1.75 inches. The first stage was partial admission and incorporated a conical De Laval nozzle. The second stage was also partial admission but contained the more conventional airfoil type converging-diverging nozzles. The third stage was full admission and contained the same type of nozzles as the second stage. Figure 6-1 illustrates the second stage stator and rotor.

Test results of the TATP I turbine indicated that the performance of this unit was considerably below expectations. Investigations indicated this poor performance was probably due to an unchoked second stage nozzle. This was attributed to assuming supersaturation up to 4% maximum during the design, and the use of perfect gas equations which assumed isentropic flow to the throat of the nozzle, to calculate the nozzle throat areas. As a result of the analysis of TATP I test results, it was decided to enlarge the first stage nozzle throat diameter to pass a larger flow at design inlet conditions. Other changes incorporated in TATP II were labyrinth seal clearances, axial nozzle-rotor clearances, nozzle chord length, and nozzle and rotor heights. Material changes in the rotor and nozzles and in package internal insulation were also accomplished.

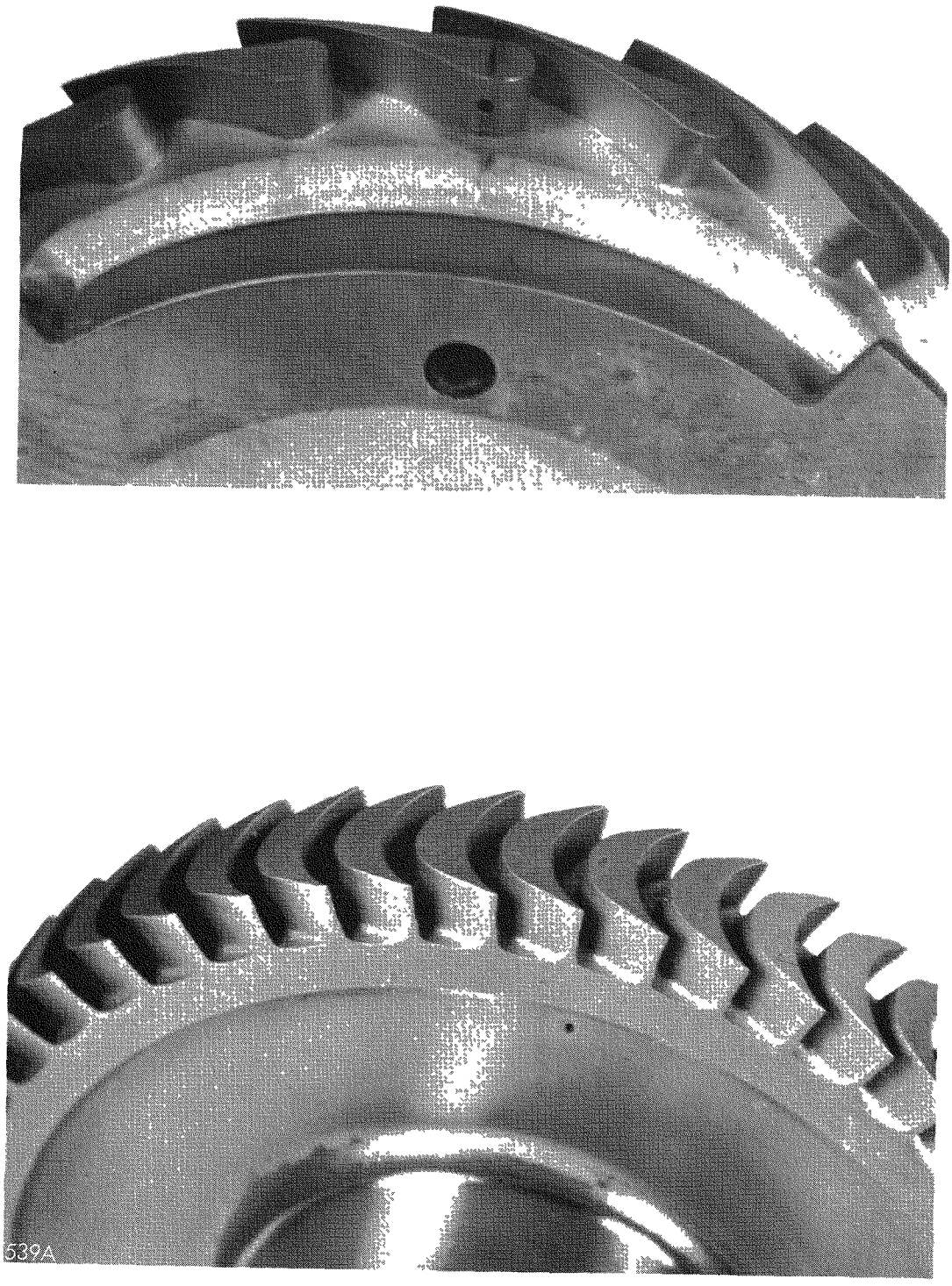

TURBINE STATOR AND ROTOR

FIGURE 6-1

6.2.1 Experimental Results

The experimental turbine data available for TATP II included a calibration of the first stage nozzle and experimental performance for rotational speeds of 20,000, 30,000, 40,000 and 45,000 rpm.

The TATP II turbine experimental performance presented in this report is a composite of data obtained from all TATP tests. Experimental turbine output power for TATP II is the summation of alternator calibration powers, pump, bearing and parasitic power absorptions. These calibrations are the results of nitrogen spindown tests performed in the TATP II package and are described in the SNAP I power conversion system report, ER-4050. The experimental aerodynamic powers for TATP II turbine, for rotational speeds of 20,000, 30,000, 40,000 and 45,000 rpm are plotted in Figure 6-2. Maximum power output is observed to be at a speed of approximately 30,000 rpm rather at the design speed of 40,000 rpm. The 20,000 rpm value of aerodynamic power is an extrapolated value since the flow and inlet conditions are not at the design values.

6.2.2 Computer Analysis

The computer off-design analysis was performed on the IBM 650 magnetic drum data processing machine, utilizing the equations of the turbine off-design program. This analysis was concerned with the simulation and verification of the experimental performance data presented in section 6.2.1 of this report. Of particular interest were the power-speed relationship and the nozzle calibrations. There was no attempt made to improve TATP II performance by hardware modifications and retesting since program scope did not permit this.

Using the experimental inlet and exhaust conditions, computer solutions were made for rotational speeds of 30,000, 40,000 and 45,000 rpm. The results of the first and second stages are plotted in Figures 6-3 and 6-4. Examination of these curves indicates that both stages 1 and 2 attain peak efficiency between 40,000 and 45,000 rpm.

A computer solution, assuming an unchoked third stage rotor, was obtained only for the 30,000 rpm run. A choked rotor was indicated at both 40,000 rpm and 45,000 rpm. In order to pass the correct flow through an unchoked third stage rotor, there must be a pressure at the rotor "exit throat" higher than the condenser pressure, and further expansion downstream of the rotor blades would occur similar to a "straight back" nozzle. An attempt was also made to determine the third stage performance by assuming a choked rotor. For both 40,000 and 45,000 rpm, this analysis could not be completed since both excessive negative incidence and very low Reynolds numbers were beyond the range of the program data. These calculations indicated a choked third stage rotor and that the third stage for the 40,000 and 45,000 rpm runs was not producing the power which would have been produced for pure impulse operation. The choked rotor condition could have been alleviated by increasing the rotor flow area, resulting in a higher level of turbine performance.

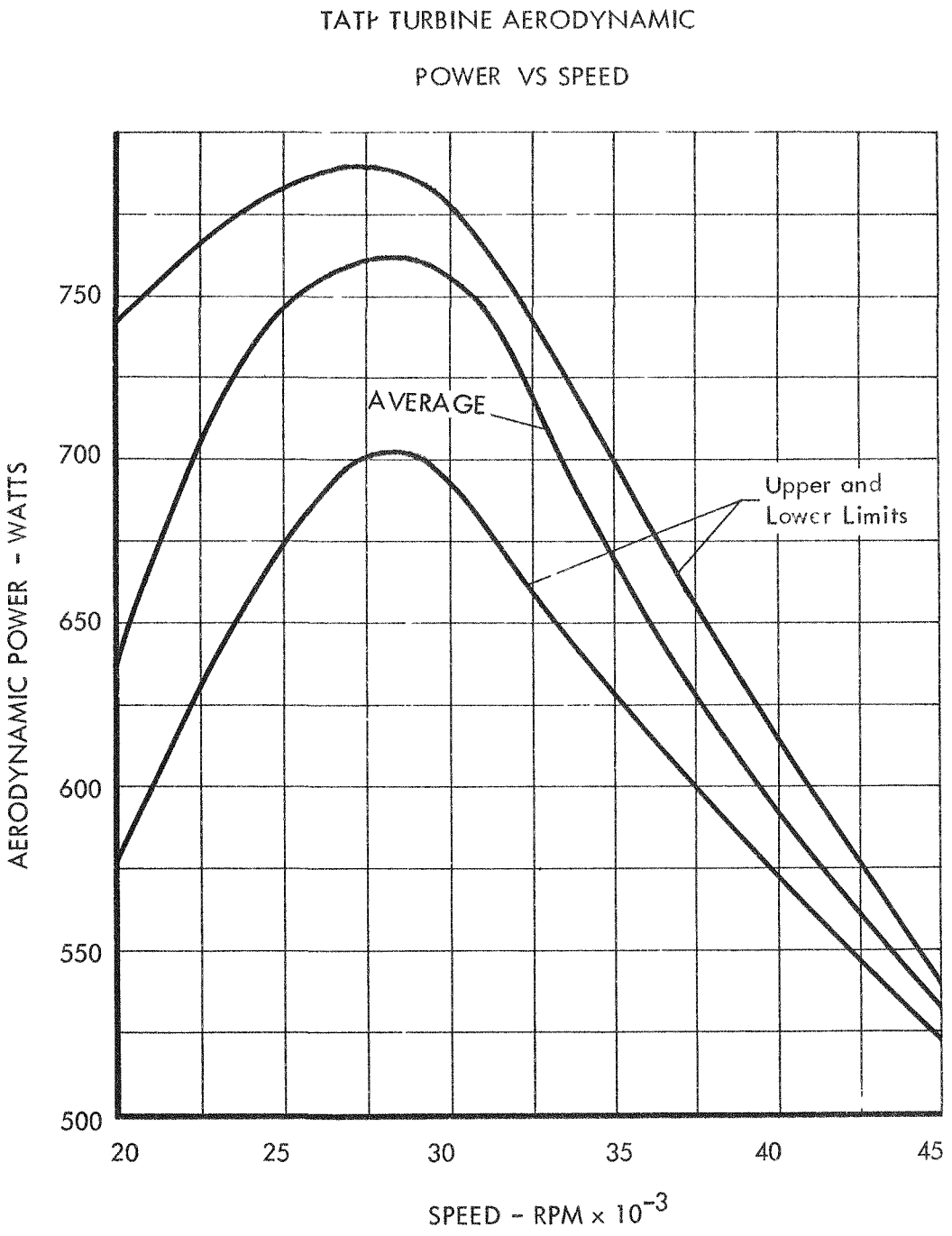
TATP TURBINE AERODYNAMIC
POWER VS SPEED
AERODYNAMIC POWER - WATTS
750
700
650
600
550
500
AVERAGE
Upper and
Lower Limits
20
25
30
35
40
45
SPEED - RPM x 10^-3

FIGURE 6-2

TATP II FIRST STAGE EFFICIENCY
VS U/C RATIO
FROM COMPUTER ANALYSIS

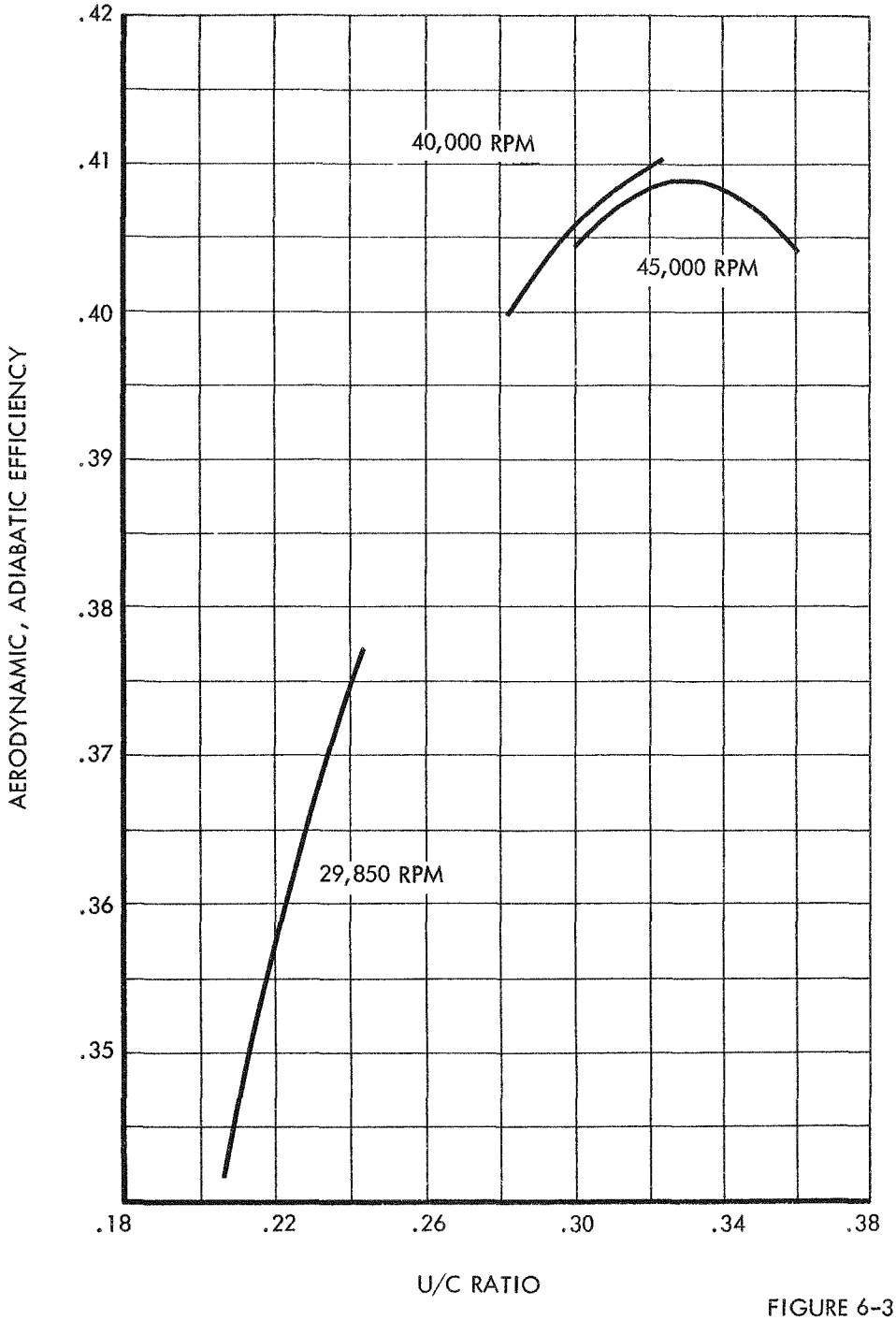

FIGURE 6-3

TATP II SECOND STAGE EFFICIENCY
VS U/C RATIO FROM COMPUTER ANALYSIS

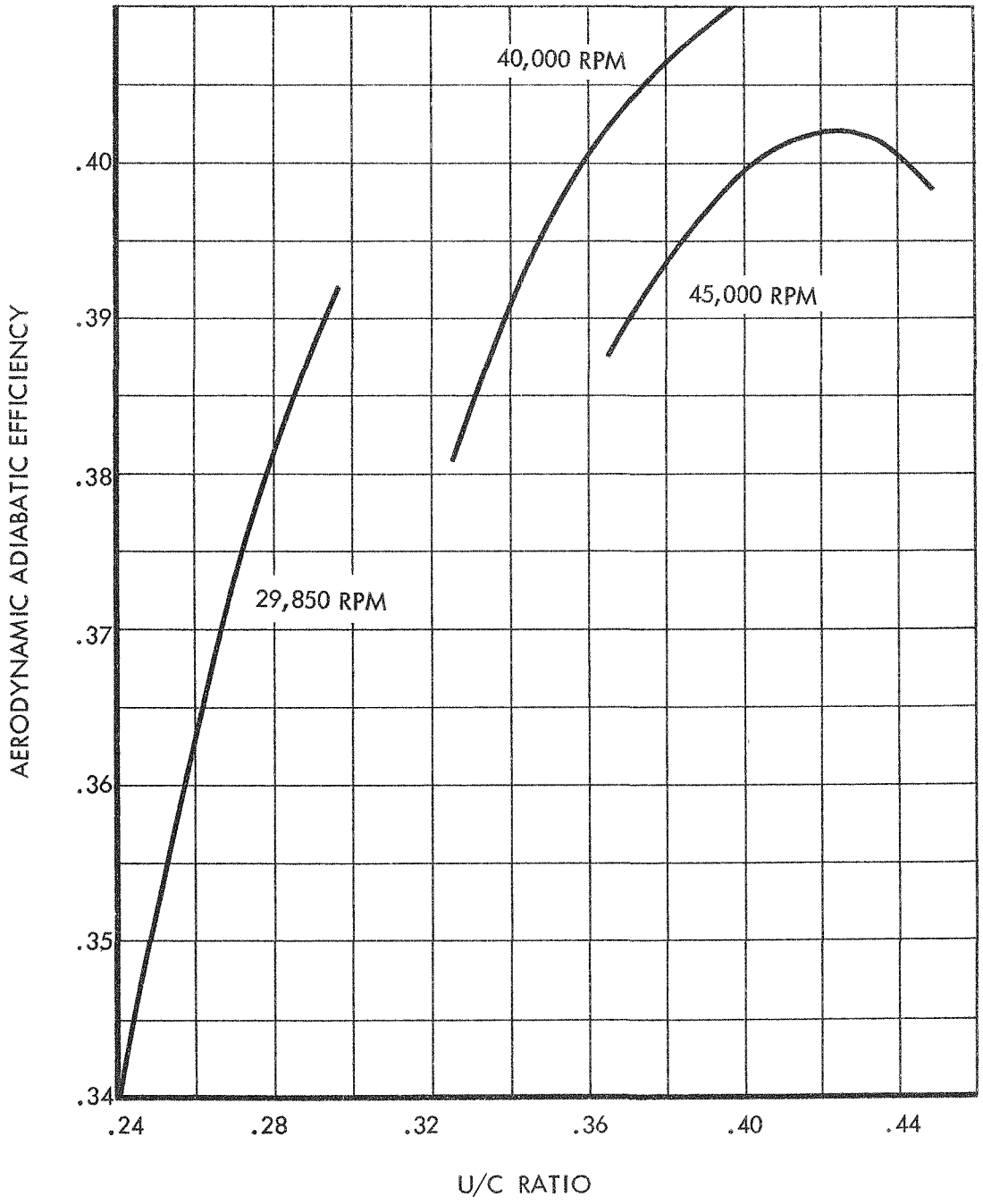

FIGURE 6-4

During the computer analysis, a discrepancy in the calculated flow and measured flow during the TATP nozzle calibration was observed. Since the TATP nozzle calibration was conducted carefully, (especially the flow measurement), the conclusion was that liquid mercury droplets or slugs were being passed through the nozzle as well as the superheated vapor. This effect would explain the large flows observed since the liquid to vapor density ratio is of the order of 300. Thus, the volumetric percentage of droplets or the area occupied by liquid at any cross-section need not be very large to produce these results.

The turbine power at various speeds was recalculated using the flows obtained from the nozzle calibration rather than the calculated flow. These results provided improved correlation with the experimental powers. The band of calculated turbine powers intersects the range of experimental results as shown in Figure 6-5. The calculated powers are for the adiabatic case and heat transferred from the turbine should be subtracted from the calculated results in order to provide a comparison with the experimental powers. A preliminary analysis indicated that the heat transfer losses were low although no detailed thermal analysis was attempted.

Any static pressure drop taken by the rotor is at the expense of the nozzle, producing an off-design condition. If the nozzle pressure drop is much less than design, as is indicated in the TATP II third stage at 40,000 and 45,000 rpm, many performance damaging effects may come into play. Losses can result from shocks occurring within the converging-diverging nozzle. In the worst case, the nozzle can become unchoked and function as a subsonic diffuser. As the spouting velocity from the nozzles decreases, the flow into the rotor is directed more towards the axis of the shaft (for constant rotational speed), possibly surpassing this and being directed against the back side of the rotor blades. This decrease in spouting velocity causes a negative incidence on the rotor blades. (A condition which has been experimentally observed to be more severe than positive incidence.) The low velocities provide low Reynolds' numbers which increase losses resulting in low efficiencies.

The indications of the static pressure drop in the rotor are to be expected since the TATP II third stage had been originally designed for a flow considerably less than was passing through the unit during these tests. It is to be expected that a pressure drop would exist when passing a greater flow through the same area.

TATP II EXPERIMENTAL AND CALCULATED POWER VS. SPEED

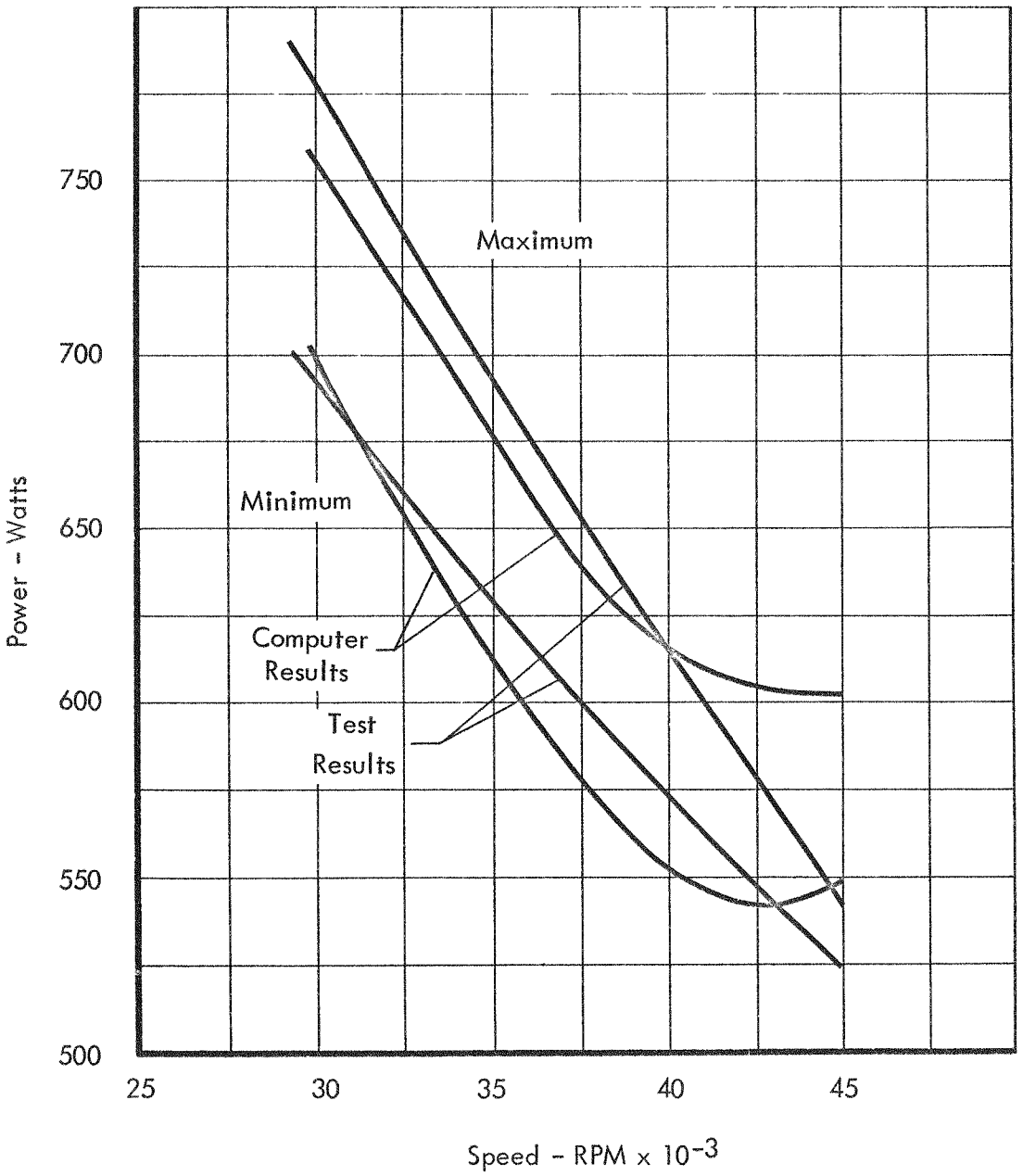

FIGURE 6-5

6.3 PTP Turbine

The results obtained from the TATP turbine test results verified the fact that mercury vapor axial flow turbines could be used efficiently for low power applications. The first complete SNAP I turbomachinery package; the Prototype Test Package (PTP), was designed to integrate the overhung jet-centrifugal mercury pump, the mercury-lubricated hydrosphere bearings, a radial gap alternator, and a three stage axial flow turbine.

Two major design considerations in the PTP turbine were: to minimize heat loss from conduction through the shaft and housing to the cooler portions of the package and the mercury bearing lubricant, and to minimize interstage and rotor blade tip leakages. Because the PTP turbine was designed utilizing the recently completed IBM 650 turbine design program, several configuration studies were completed in order to optimize the design. It was also possible to design the turbine so that slightly off design conditions would not produce appreciable losses in turbine performance.

Since the PTP was intended to evaluate system performance, instrumentation was not provided for detailed component evaluation. Over-all experimental results did show, however, that the maximum efficiency occurred at the design speed of 40,000 RPM and the turbine met the minimum design requirements. An investigation of the fabricated turbine geometry revealed that the third stage nozzle blade height of the only package tested (PTP-1) was oversized. This resulted in an off design third stage and a lower power output than had been anticipated. In spite of this, the turbine still met its specifications. Correction of these fabrication errors in subsequent turbines would improve the design point performance.

Since limited turbine experimental data was available from the PTP-1 test results, it was decided to simulate the test runs utilizing the IBM 650 turbine off-design program.

The off-design analysis was made to determine more accurately the performance parameters of the PTP-1 package, and to consider improvements to be incorporated into the PTP-2 package at minimum cost and rework.

The analysis indicated that the original PTP turbine was still the best design for the conditions and specifications originally outlined. A slight improvement might be realized by reducing the third stage blade height slightly from its design value. It was therefore, decided to remain with the original design since project funds at this time were greatly reduced.

6.3.1 Experimental Results

Instrumentation on the PTP turbine was limited to total temperature and total pressure at the inlet of the turbine, static pressure at the first stage nozzle exit, and static pressure and temperature at the turbine exit. The turbine speed was obtained from the alternator

frequency. Because of this there could be no precise experimental values of powers or efficiencies for the PTP turbine. Package instrumentation enabled determination of turbine flow, ideal enthalpy drop, and thus turbine ideal power. The experimental turbine powers and efficiencies were obtained from a knowledge of alternator output and power consumption of the pump, bearings, and alternator.

Plots of turbine aerodynamic efficiency vs speed in Figure 6-6 show the range of values and an arithmetic average of points at each speed. It can be seen that the peak total-to-static efficiency occurred in the vicinity of 40,000 rpm at an average value of 42%. The corresponding output power was 682 watts. Table 6-1 is a comparison of experimental and predicted turbine performance at 40,000 rpm for PTP-1.

6.3.2 Computer Analysis

Using the turbine inlet and exhaust conditions and turbine geometry, an IBM 650 computer off design analysis was made of the PTP-1 turbine performance at the following cycle conditions:

Inlet total. Pressure	206.4 psia
Inlet total Temperature	1283°F
Exhaust Static Pressure	1.92 psia
Speed	40,000 rpm

The results desired from this analysis were correlation of experimental and calculated results and determination of design changes which would improve the performance of the unit. Design revisions to be considered were as follows:

1) Incorporate changes in turbine nozzle area so as to optimize the present turbine output and, if necessary, make minor changes in rotor blade geometry and wheel diameter.

2) Improve turbine power output by reducing running clearances, such as the rotor radial tip clearances and the high pressure and first interstage labyrinth clearances.

Since program funding did not allow extensive hardware modifications to be made, effort was directed towards determination of the best possible unit utilizing hardware with minor modifications.

In view of the foregoing, it was decided to investigate the following possibilities:

Number of second stage nozzle passages - 7 (design)
- 6
- 5

ESTIMATED TURBINE AERODYNAMIC EFFICIENCY
VERSUS ROTATIONAL SPEED

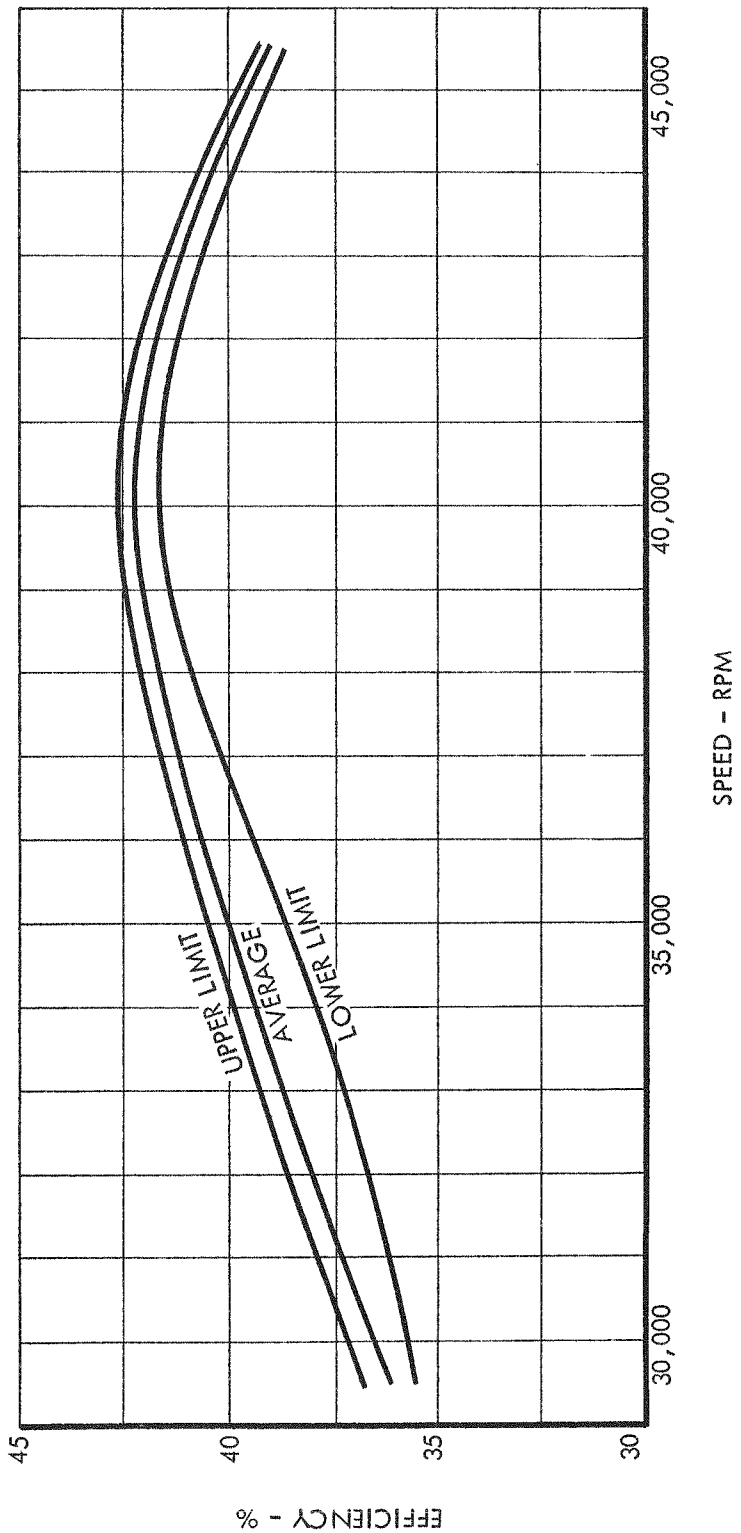

FIGURE 6-6

TABLE 6-1

COMPARISON OF EXPERIMENTAL AND DESIGN SPECIFICATION PERFORMANCE FOR PTP-1 TURBINE

	Experimental Range	Experimental Average	Design Specification
Inlet Total Pressure, psia	206-211	208	210
Inlet Total Temperature ^{o}F	1280-1296	1289	1300
Rotation Speed, rpm	40,000-40,100	40,020	40,000
$P_{exhaust}$, psia	1.77-2.44	2.04	2.06
Turbine Flow, lb/sec	.0305-.0311	.0308	.0311
Aerodynamic Power, watts	660.8-700.5	682	654
Aerodynamic Efficiency, %	41.6-42.7	42	40

Third stage nozzle blade heights
- .1250 inch
- .1135 inch (design)
- .080 inch

These variations in the 2nd and 3rd stage nozzles would produce changes in the passage areas and result in different pressure distributions throughout the three stage turbine. A more favorable pressure distribution would improve turbine performance. The actual fabricated PTP-1 turbine contained seven nozzle passages in the second stage and a third stage nozzle blade height of .1250 inch. This greater than design blade height was due to a machining error that was not corrected due to the reduced program status at that time.

The turbine analysis was performed on the IBM 650 computer using the equations of the turbine off-design program. The analysis was not meant to be refined, but rather to indicate the directions in which improvement was to be found. The first calculations assumed that the third stage nozzle was choked. Additional computer runs were made for an unchoked third stage nozzle.

The total powers for the turbine combinations were then plotted as shown in Figure 6-7. This figure consists of three curves, one for each possible second stage with varying third stage nozzle blade heights. Of the combinations analyzed, the best configuration was the PTP turbine as designed with 7 second stage nozzles and a third stage blade height of .1135".

The maximum power may be obtained by a slight reduction in third stage nozzle blade height from the original design. However, it cannot be accurately determined whether the plugging of the third stage nozzle would have the same effect as lowering the blade height to approximately .102 in. The effect of the partial admission on the third stage, which was designed to have reaction in the rotor, is very uncertain. Further optimization would be found only in extrapolation of the results shown and a major design revision.

In the analysis for the unchoked third stage condition, excessive incidence was encountered at the inlet to the third stage rotor. Since the values were out of the range of the cascade test data, the solution could not be obtained. The flow incident angle on the rotor in some cases was so adverse that it left doubt as to whether the rotor was providing power or absorbing power. It was felt that with the severe incidence condition, the best alternative would be to assume no power output from the third stage and take the additional pressure drop in the second stage.

If 60 watts heat transfer is subtracted from the values of 736 watts (for 7 nozzles) shown in Figure 6-7, the aerodynamic power of 676 watts correlates well with the experimental average value obtained previously (682 watts). Thus, the third stage nozzle of PTP-1 turbine was apparently unchoked, and performance improvement could be gained by decreasing the critical area of the third stage nozzle, preferably by decreasing the nozzle

PTP TURBINE POWER AS A FUNCTION OF THIRD STAGE NOZZLE BLADE HEIGHT AND NUMBER OF SECOND STAGE NOZZLE PASSAGES

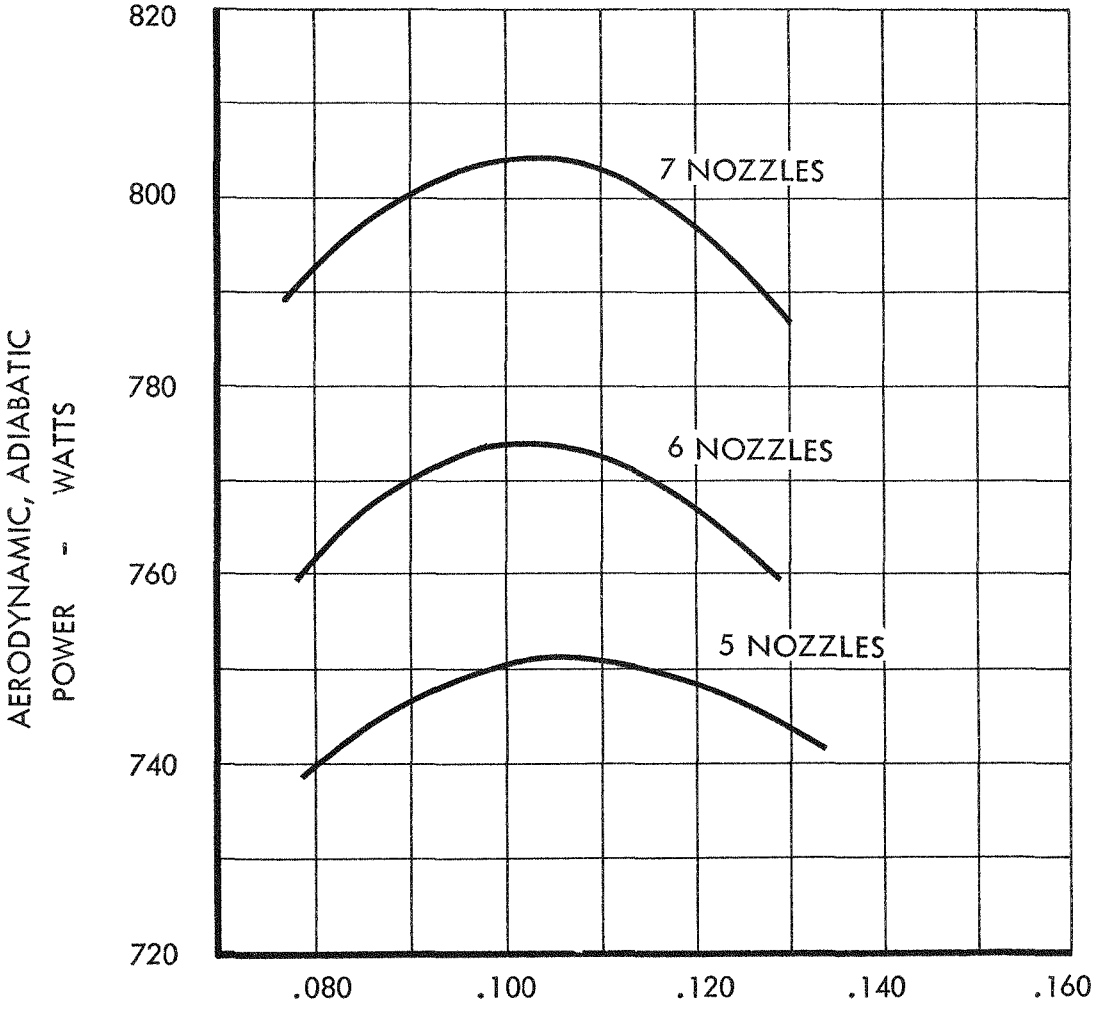

FIGURE 6-7

blade height from the .1250 inch nozzle installed in PTP-1 to the design value of .1135 inch.

Based on this study, modifications were made to the turbine of the second prototype turbomachinery package fabricated. Unfortunately, it was not possible to test this unit (PTP-2) sufficiently to provide data enabling a performance comparison with PTP-1 to be made. All of the PTP turbine performance and endurance data was obtained with PTP-1. As well as the performance achievements discussed above, this unit operated for 3 1/2 months at full speed and full power. No decay in performance was apparent during this endurance run, indicating that the SNAP I turbine design is also highly satisfactory with respect to life.

7.0 TURBINE TEST FACILITIES

The preliminary testing of the SNAP I turbine was accomplished with steam and air as the working fluid in a turbine component test facility. This test facility was utilized for all of the turbine component experimental development. The final 3-stage axial flow turbine was evaluated from mercury vapor tests of the system test packages operated in special system test facilities.

Figure 7-1 is a photograph of the SNAP I turbine test facility showing the instrumentation and control console on the left and the turbine dynamometer stand on the right. Also part of the facility was the steam supply and exhaust systems and the high temperature air supply system.

7.1 Steam Turbine Test Rig

The steam turbine test facility included a steam supply and exhaust system, and the turbine dynamometer, instrumentation, auxiliary equipment, and control consoles shown in Figure 7-1. The turbine dynamometer assembly consisted of a drag turbine and an air absorption dynamometer mounted on oil-lubricated bearings. The turbine wheel was mounted directly on the shaft of the high speed fan-type absorption dynamometer which was designed for this application.

An optical pickup provided the actuating electrical output for speed measurement and a load cell incorporating a proving ring and a differential transformer provided the actuating electrical output for torque measurement. The steam flow measurement was obtained by observing the pressure drop across a calibrated thin plate orifice. A throttling calorimeter was installed in the inlet line to determine steam quality at the nozzle inlet. Total temperature thermocouple probes were inserted in the steam flow path to measure main line, nozzle inlet, turbine outlet, and diffuser exhaust total temperatures. Total pressure probes were installed at the nozzle inlet, turbine outlet and diffuser exhaust. Static pressure taps were located in the main line, nozzle inlet, turbine outlet, diffuser exhaust, and five peripheral points around the turbine scroll. Mercury manometers were employed for the measurement of all total and static pressures and thermally insulated steam pots with overflows were installed for the collection of condensate to eliminate pressure corrections due to the liquid head of the condensate.

7.2 Air Turbine Test Rig

Development testing of the various turbine designs was also conducted with air as the working fluid. A preference was given to air since higher pressure ratios could be developed with existing laboratory facilities. The data from the air tests was the basis for predicting turbine performance with mercury by use of dynamic similarity techniques.

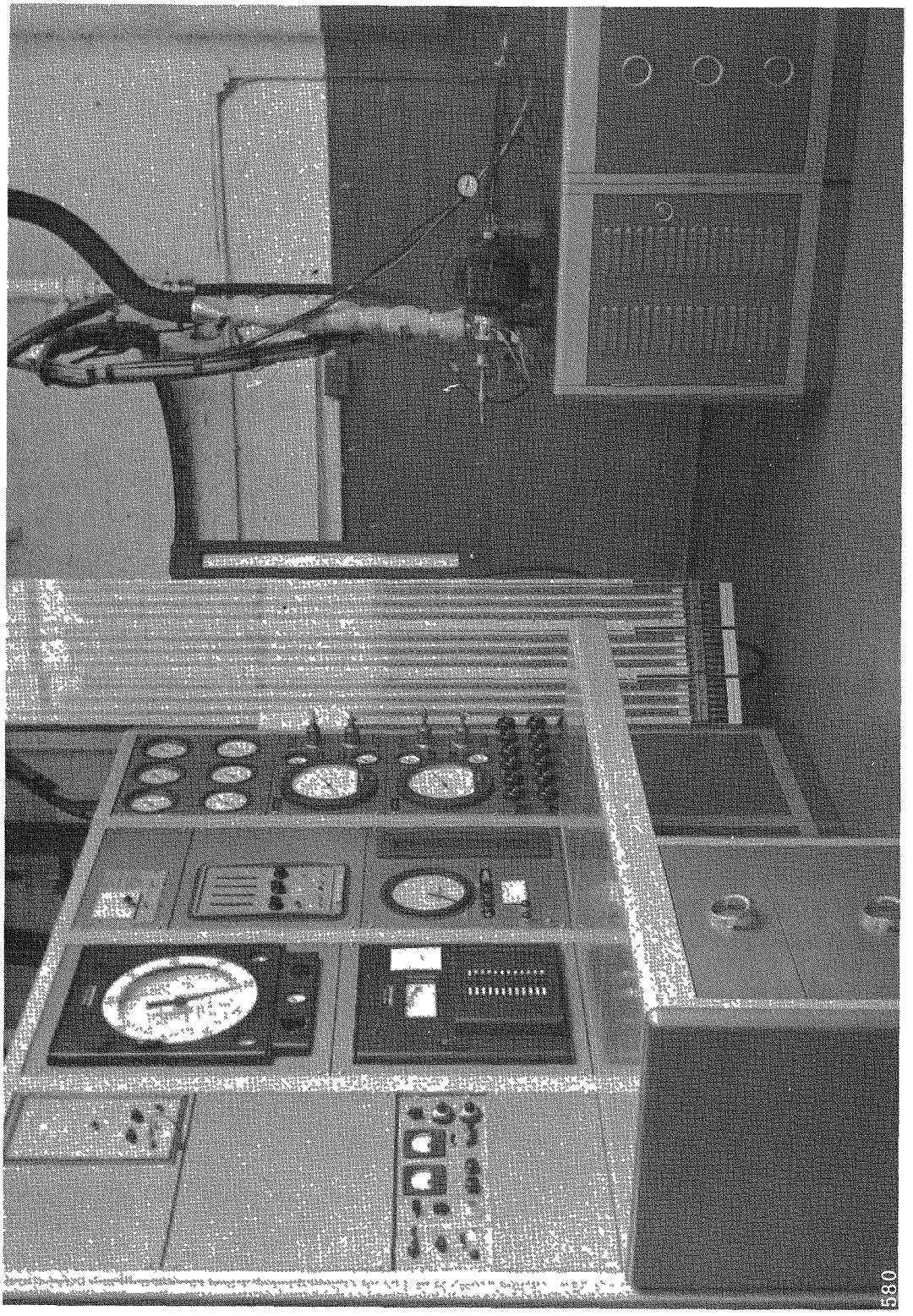

AIR AND STEAM TURBINE TEST RIG

FIGURE 7-1

The air turbine test facility was obtained by modification of the existing steam turbine test rig. An electrically heated line from a booster compressor provided turbine inlet gas at pressures to 220 psia and temperatures to 1300°F.

The completely equipped test facility was available for the cold and hot gas testing of small turbines. This facility included a high speed absorption type fan dynamometer, shown in Figure 7-2, which was capable of speeds to 60,000 rpm and of power absorption to 10 horsepower. A complete complement of indicating and of recording equipment is available to monitor and to record the following parameters: temperatures, pressures, flow, rotational speeds, and torque outputs.

A magnetic pickup and electronic counter replaced the optical pickup and electrical indicating meter for speed indication. The air flow measurement was obtained by observing the pressure drop across a calibrated thin-plate orifice. Bourdon-type pressure gauges were installed for the high pressures and mercury manometers for the measurement of the lower pressures.

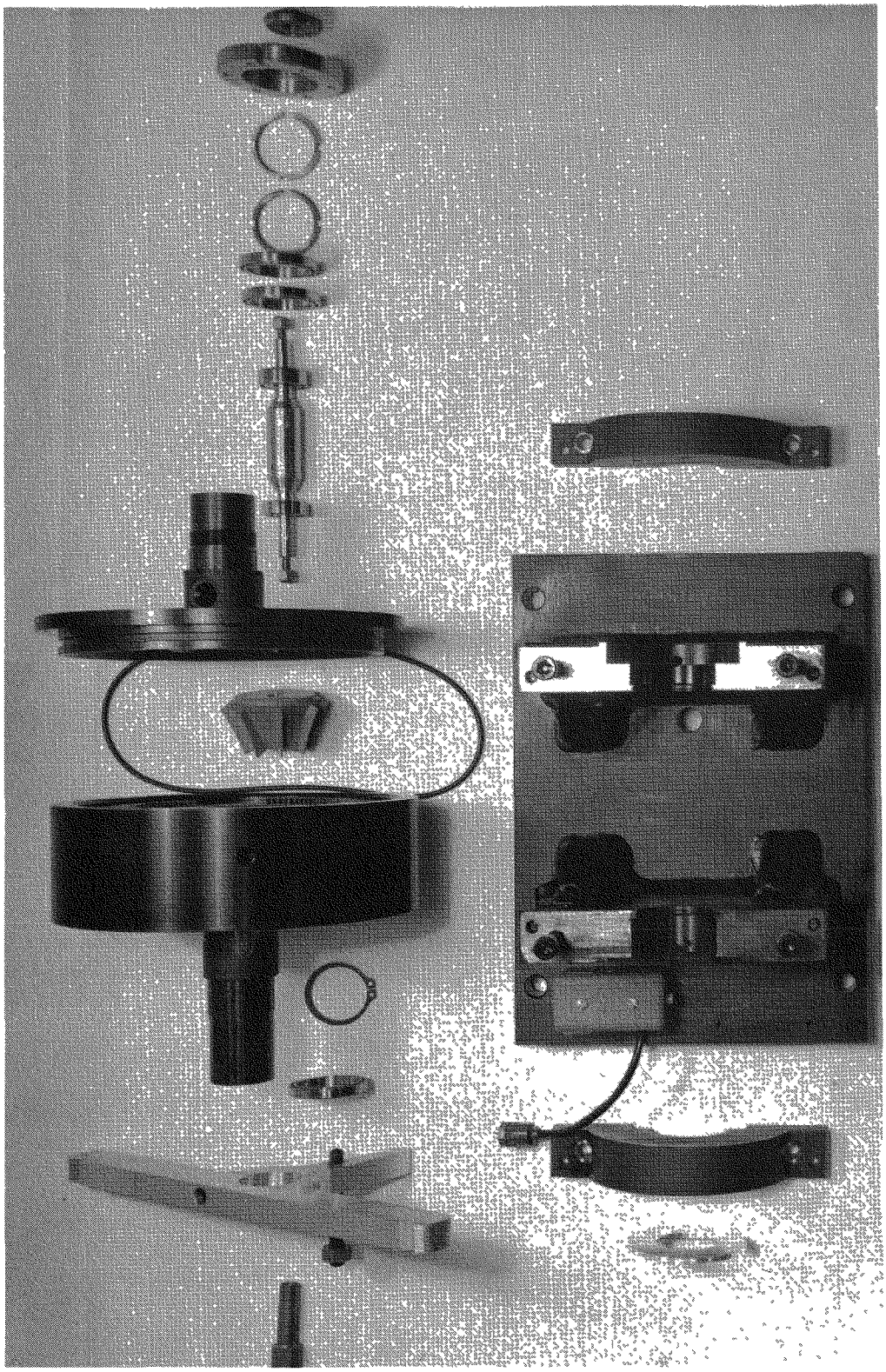

ABSORPTION FAN DYNAMOMETER

FIGURE 7-2

8.0 CONCLUSIONS

The final mercury turbine which satisfied the requirements of the SNAP I system consisted of a three stage axial flow turbine with the first two impulse stages partial admission and the last stage full admission with a slight amount of reaction.

Analytical and empirical axial flow turbine design procedures were evolved and verified by experimental testing for low specific speed, erosion limited, small size, mercury vapor turbines.

The axial flow turbine was successfully integrated into the turbomachinery package of the prototype power conversion system.

The final SNAP I turbine developed 682 watts of shaft power with an efficiency of 42 percent at the design rotational speed of 40,000 RPM. This performance was obtained during system tests and exceeded the required design specifications.

Endurance testing of the SNAP I turbomachinery package in the power conversion system exceeded the life requirement of 60 days successful operation. For 2510 hours operation was obtained with no degradation of turbine performance.

Evaluation of the regenerative-type turbines revealed relatively low efficiencies and indicated that extensive development would be necessary to obtain the performance required in the SNAP I application.

The analytical equations and the experimental test results for power output and efficiency of the regenerative-type turbines show a reasonable correlation.

Experimental drag turbine efficiencies of approximately 22% were obtained with steam and approximately 13% with air.

Experimental air vortex turbine efficiencies of 21% were obtained with a smooth turbine scroll. The addition of re-entry vanes in the turbine scroll decreased the over-all efficiency.

REFERENCES AND BIBLIOGRAPHY

The reports listed in the bibliography are not available for general distribution. Any inquiries concerning the availability of this information should be directed to the AEC.

SPTP Turbine Design	11/10/58	J. A. Matz	Secret
TM 1373 TATP II First Stage Conical Nozzle Calibration	3/19/59		Secret
TM 1390 SPTP First Stage Nozzle Calibration	5/8/59		Secret
TM 1435 Analysis of PTP #1 Turbine	7/8/59		Secret
TM 1457 SNAP I Turbine Development Program	8/25/59		Secret
TM 1459 Evaluation of TATP II Turbine	9/1/59		Secret